



1-1-2018

Development Of A Geological And Oil Reservoir Numerical Simulation Model To Predict The Effectiveness Of Surfactant Imbibition Enhanced Oil Recovery For The Bakken Formation In North Dakota

Stephen Lockwood Detwiler

[How does access to this work benefit you? Let us know!](#)

Follow this and additional works at: <https://commons.und.edu/theses>

Recommended Citation

Detwiler, Stephen Lockwood, "Development Of A Geological And Oil Reservoir Numerical Simulation Model To Predict The Effectiveness Of Surfactant Imbibition Enhanced Oil Recovery For The Bakken Formation In North Dakota" (2018). *Theses and Dissertations*. 2197.
<https://commons.und.edu/theses/2197>

This Thesis is brought to you for free and open access by the Theses, Dissertations, and Senior Projects at UND Scholarly Commons. It has been accepted for inclusion in Theses and Dissertations by an authorized administrator of UND Scholarly Commons. For more information, please contact und.common@library.und.edu.

DEVELOPMENT OF A GEOLOGICAL AND OIL RESERVOIR NUMERICAL
SIMULATION MODEL TO PREDICT THE EFFECTIVENESS OF SURFACTANT
IMBIBITION ENHANCED OIL RECOVERY FOR THE BAKKEN FORMATION IN NORTH
DAKOTA

by

Stephen Lockwood Detwiler
Bachelor of Arts, Albion College, 2014

A Thesis
Submitted to the Graduate Faculty

of the

University of North Dakota

in partial fulfillment of the requirements

for the degree of


Masters of Science
Geological Engineering

Grand Forks, North Dakota


August
2018

© 2018 Stephen Detwiler

This thesis, submitted by Stephen Lockwood Detwiler in partial fulfillment of the requirements for the Degree of Master of Science Geologic Engineering from the University of North Dakota, has been read by the Faculty Advisory Committee under whom the work has been done and is hereby approved.



Dongmei Wang 2/12/18




Stephan Nordeng 7/12/18

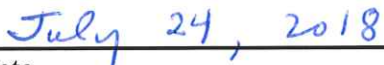


I-Hsuan Ho 7/12/18

This thesis is being submitted by the appointed advisory committee as having met all of the requirements of the School of Graduate Studies at the University of North Dakota and is hereby approved.



Grant McGimpsey
Dean of the School of Graduate Studies



Date

PERMISSION

Title Development of a Geological and Oil Reservoir Numerical Simulation Model to Predict the Effectiveness of Surfactant Imbibition Enhance Oil Recovery for the Bakken Formation in North Dakota

Department Harold Hamm School of Geology & Geological Engineering

Degree Master of Science Geological Engineering

In presenting this thesis in partial fulfillment of the requirements for a graduate degree from the University of North Dakota, I agree that the library of this University shall make it freely available for inspection. I further agree that permission for extensive copying for scholarly purposes may be granted by the professor who supervised my thesis work or, in her absence, by the Chairperson of the department or the dean of the School of Graduate Studies. It is understood that any copying or publication or other use of this thesis or part thereof for financial gain shall not be allowed without my written permission. It is also understood that due recognition shall be given to me and to the University of North Dakota in any scholarly use which may be made of any material in my thesis.



Stephen Detwiler

Date 7/10/18

TABLE OF CONTENTS

LIST OF FIGURES	vi
LIST OF TABLES	vii
ACKNOWLEDGMENTS	viii
ABSTRACT	ix
CHAPTERS	
I. INTRODUCTION	1
1.1 Geology Background of Bakken Formation.....	1
1.2 Bakken Petroleum System Background	3
1.3 Oil Recovery History of Bakken Wells and Proposed EOR Method...	6
1.4 Hypothesis.....	11
II. METHOD	12
Phase 1: Data Collection	13
Phase 2: Geologic Modeling	15
Phase 3: Production History Matching.....	19
Phase 4: Surfactant Imbibition and Effectiveness Forecasting.....	22
III. RESULTS	23
IV. DISCUSSION	33
Conclusion.....	40
Nomenclature.....	41

REFERENCES.....	42
APPENDICES.....	45

LIST OF FIGURES

Figure	Page
1. Figure 1.1: Representation of the Bakken in relation to stratigraphic succession, geologic time and lithology of member units. Grey = shale, yellow = dolostone, dark blue= shoal (low porosity limestone), light blue = limestone (porous), and orange = siltstone.....	1
2. Figure 1.2: Reconstruction of North America in Late Devonian to Early Mississippian. Red outline represents estimated location of Williston Basin at this time. (Modified from Blakey, 2011).....	3
3. Figure 1.3: Oil bearing formation event timeline for the Bakken Formation (Pollastro et al., 2010).....	4
4. Figure 1.4: USA extent of the Bakken Formation. Depicts structural features from previous deformations. Solid black oval areas are general locations of oil production (1) Antelope field, (2) Elm Coulee Field, (3) Parshall and Sanish Field. (Pollastro et al, 2010).....	5
5. Figure 1.5: Burial History curve of three well locations in the Willison Basin North Dakota. Well names and file numbers located to top left of each curve set. Colors on burial curves represent calculated transformation ratios with respect to burial depth, time, and temperature. Bold line represent the Bakken Formation. Dashed line is the 50Ma age (modified from Pollastro et al. 2010).....	6
6. Figure 1.6: Top to bottom, Nonionic, Anionic, Cationic, and Amphoteric Surfactant molecules (Modified from Malmsten, 2002).....	8
7. Figure 2.1: Initial workflow of how to construct a geological model and Oil reservoir simulation model.....	12
8. Figure 2.2: Map of Mountrail County with the 24 wells used for 3D modeling. Yellow highlighted area is the extent of the area that will be 3D modeled.....	13
9. Figure 2.3: Map of North Dakota and the modeled area used in geological modeling –GES2016. Area comprises of Eastern half of Mountrail County. There are a total of 24 wells and nine Cross sections made for well correlations. The red highlighted area is the extent of the model used in numerical simulation – CMG-STARS	16

10. Figure 2.4: Reference Section of well #15845. Section includes Petrophysical data (Starting left to right) on Gamma ray signature, SSTVD Depth in feet, NPOR and DPHZ signatures, and Lithology classification based on Petrophysical Data. Zones were established based on reoccurring patterns seen in all wells from cross section correlations.....	17
11. Figure 2.5: Production history of Patten 1-27H Well # 16799. Data provided from North Dakota DMR website (DMR, 2018)	20
12. Figure 3.1: Contour map of Eastern Mountrail County generated in ArcGIS from 610 wells within and surrounding Mountrail County. Tops were selected and corrected from Kelly Bushings readings from data provided by DMR, 2018. Constructed with Empirical Bayesian Kriging (EBK). Top contour represents the top of the Bakken Fm., bottom contour represents the top of the Three Forks Fm. Highlighted wells represent the 24 wells with necessary petrophysical data used for geologic modeling.....	23
13. Figure 3.2: Structural well correlation of (from left to right) wells # 17676, 99186, 16824, 21928, 16997, 99188. Cross section matches with A-A' cross sections seen in Figure 2.3.....	25
14. Figure 3.3: Cross Section along the trajectory of Well #16799. Cross section represents the lithofacies. Grey = Shale, Green = Dolostone, Blue = Limestone, Pink = Shoal, Orange = Gamma High Dolostone. Vertical trajectory is the pilot trajectory used for modeling, Horizontal trajectory was used for Contour correcting.....	26
15. Figure 3.4: Core Comparison and Thin section observation of Bakken Rock in Core 15845. Gamma Ray, Neutron Porosity, and Density Porosity data (DMR, 2018). 5 zones of Lithofacies were generated from bottom to top are Zone 1: Lower Bakken Shale, Zone 2: lower-Middle Bakken limestone, Zone 3: central-Middle Bakken, Zone 4: upper-Middle Bakken dolostone, and Zone 5: Upper Bakken Shale. Core and thin section photos provided by UND Core library.	27
16. Figure 3.5: 3D view of east Mountrial County Bakken Formation. Lowest corner represents the SW corner of field area. Models show lithology, porosity, water saturation (Sw) and permeability (True Perm). All images are a 50x vertical exaggeration of elevation.....	28
17. Figure 3.6: Placement and trajectory path of Well # 16799 in CMG. Map view of the numerical simulation grid is the image to the left and a side view of the numerical simulation grid is the image to the right.....	28

18. Figure 3.7: Comparison field data to simulation data for cumulative oil produced and water cut percentage. Circle symbol = real world cumulative oil production data, square symbol = real world water cut % data, red solid lines = simulated cumulative oil production data, and blue dashed line= simulated water cut % data.....	29
19. Figure 3.8: Comparison of surfactant concentrations of 0.1%, 0.5%, and 1.0% of Wang et al, 2012 nonionic surfactant formulation. The “continued production” curve is a projection of current production of the system. The “water injection” curve is modeled similar to surfactant injection, but with 0% surfactant concentration. All scenarios, expect for continued production, used 30-day injection, 15-day Shut in period, and 90-day production intervals.....	30
20. Figure 3.9: Comparison of different injection plans. Inj. = # of days of injection, Shut = # of days when well is completely shut to allow for surfactant permeation, Prod. = # of days the well is open for production. All injections of surfactant were done with 1.0% concentration.....	30
21. Figure 3.10: Sensitivity analysis of bottom hole pressures (BHP), width of fractures in I-direction (DI FRAC), permeability of fractures (PERM FRAC), Permeability of all cells, porosity of fractures (POR FRAC), porosity of all cells, water saturation of system, and reservoir pressure at depth. The fractures used in the model were based on natural fractures.....	32
22. Figure 4.1: Comparison of corrected shale porosity vs. non-corrected shale porosity. Red and green curves are simulation results of oil accumulation and red circles represent field data cumulative results. Dark and light blue curves are simulation results of water cut percentage and blue squares are field data water cut percentage.....	38

LIST OF TABLES

Table	Page
1. Table 2.1: Parameters for generating the 3D model in GES2016 of east Mountrail County, ND.....	19
2. Table 2.2: Averages of values generated for geological model and numerical simulation.....	22
3. Table 3.1: shows equations (2-4) constant values used for log data calculations and cell value generation.....	24
4. Table 3.2: represents bottom hole pressure from Hunt Oil Co. data and equation 4, Bolded values are the BHP needed to history match to production data.....	25
5. Table 3.3: Final number of cumulative oil production and oil recovery factors for all forecasting scenarios. Numbers in parenthesis are Injection time, Shut in time, and production time respectively.....	31
6. Table 4.1: Cost and profit comparison of implementing surfactant EOR strategies. Costs were generated from averages of installing and running fluid injection systems from US Department of Energy (Godec, 2014). Gross profit is the profit accumulated above the continuous production forecast.....	40

ACKNOWLEDGMENTS

I would like to thank Hunt Oil Company (Dallas, Texas) for providing production data. I thank Golden Sun Petroleum Technologies (Houston, Texas) and CMG for providing their software. I also thank, the Core Library at the University of North Dakota for allowing us to use their facilities for core analysis work. I thank the Harold Hamm School of Geology and Geologic Engineering faculty and staff for their education and financial support. Finally, I thank all my committee members, Dr. Dongmei Wang, Dr. Stephan Nordeng, and Dr. I-Hsuan Ho, for their time and energy in helping me complete this research.

To my loving and supporting
Parents George and Lynn,
Brother Alex,
And my wonderful wife
Rachel.

I love you all so much!

ABSTRACT

This research employs an integrated geological modeling and numerical simulation method on an ultra-tight rock formation to determine if the surfactant imbibition process is a feasible enhanced oil recovery method. The ultra-tight rock formation studied was the Bakken Formation in East Mountrail County, North Dakota. A detailed geological model and numerical simulation model of the formation was established by various technologies, e.g. ArcGIS 10.4, Geologic Evaluation System (GES2016), and Computer Modeling Group (CMG) – STARS programs. All data was collected from actual field measurements and well-log readings of in place formations. The reservoir model provided a 500 ft. × 500 ft. grid resolution 3D model of the Bakken Formation with 20-layer vertical resolution showing the formation lithology and petrophysical property distributions. The analysis of the reservoir numerical simulation model was focused on Well Patten 1-27H #16799 from Hunt Oil Company. The results from the simulation produced a production history match in oil production and water cut histories along with forecasting results. An ethoxy-sulfate alcohol nonionic surfactant of 0.1% formulation was the basis concentration and was able to simulate an increase in production of Well # 16799 by about 800,000 ft³ of oil and an incremental oil recovery factor of 9.8% OOIP compared to using current hydraulic fracturing method. In summery the simulation of huff-n-puff surfactant imbibition produced similar results found in lab core sample testing. This outcome suggests that future field-testing of surfactant imbibition enhance oil recovery is needed in order to support or modify the results found in this research.

CHAPTER I

Introduction

1.1 Geology Background of Bakken Formation

In 2008, the Bakken Formation in North Dakota's Williston Basin had a boom of oil production with the advent of horizontal drilling and fracking (Nordeng, 2010). The Bakken stratigraphy is made of four members: Upper Bakken Shale, Middle Bakken silty dolostone/limestone (mixed siliciclastic carbonates), Lower Bakken shale and Pronghorn member siltstone (Figure 1.1) (Lefever et al, 2013).

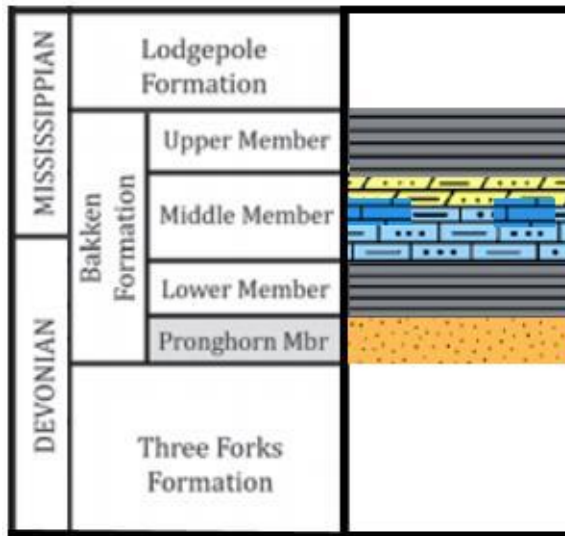


Figure 1.1: Representation of the Bakken in relation to stratigraphic succession, geologic time and lithology of member units. Grey = shale, yellow = dolostone, dark blue = shoal (low porosity limestone), light blue = limestone (porous), and orange = siltstone.

The Bakken's depositional history is comprised mostly of marine and subtidal environments. It begins with the Pronghorn as a shoreface deposit of siltstone and minor sandstone, just after the deposition of the regional unconformity Three Forks Formation (Lefever et al. 2013). Locations where the Pronghorn member deposits are thick (near the Heart River

fault) transgressive sequence from siltstone to brachiopod rich mudstone (nearshore) to open marine limestone (Lefever et al, 2013). The Pronghorn member is not seen throughout the entire extent of the Bakken Formation. In areas where it is absent, the Threeforks Fm. to Lower Bakken member contact is abrupt and unconformable (Lefever et al. 2013).

Following the Pronghorn is a transgressive rise in sea level and the deposition of the Lower Bakken Shale (Smith et al. 2000, Pitman et al 2001, and Sonnenberg 2017). The shale was deposited in an offshore marine environment (Smith et al, 2000).

After the deposition of the Lower Bakken Shale a regression of sea level causes deposition of the Middle member of the Bakken (Smith et al. 2000, Pitman et al 2001, and Sonnenberg 2017). The Middle Member is more complex; its lithology changes as sea level regression occurs. First depositing silty limestones, then possible shoal deposits. The shoal layers are large mounds of marine deposition that will break wave action early for shoreline deposition, usually found on continental shelves. These deposits tend to be fairly clean (low gamma ray signature) and low porosity limestones or clean sandstones. The shoal is a layer not always present in marine environments which is indicative of its depositional process. After the possible shoal deposition follows another deposition of silty limestone, which often is later dolomitized as a secondary process, leaving a dolostone lithology in the upper Middle Bakken.

Following the Middle Bakken is a transgression to the Upper Bakken Shale which is lithologically similar to the Lower Bakken Shale (Lefever et al. 2011).

The paleo-reconstruction model of North America, from Blakey, 2013 in Figure 1.2, displays the environments present in the USA during late Devonian and early Mississippian. As Figure 1.2 displays, there is a large marine environment in what will be North Dakota and that North America was centralized over the equator. Additionally, a depression is formed with

accommodation space for much more sediment to deposit into and allowing for proper burial/overburden conditions for oil generation.

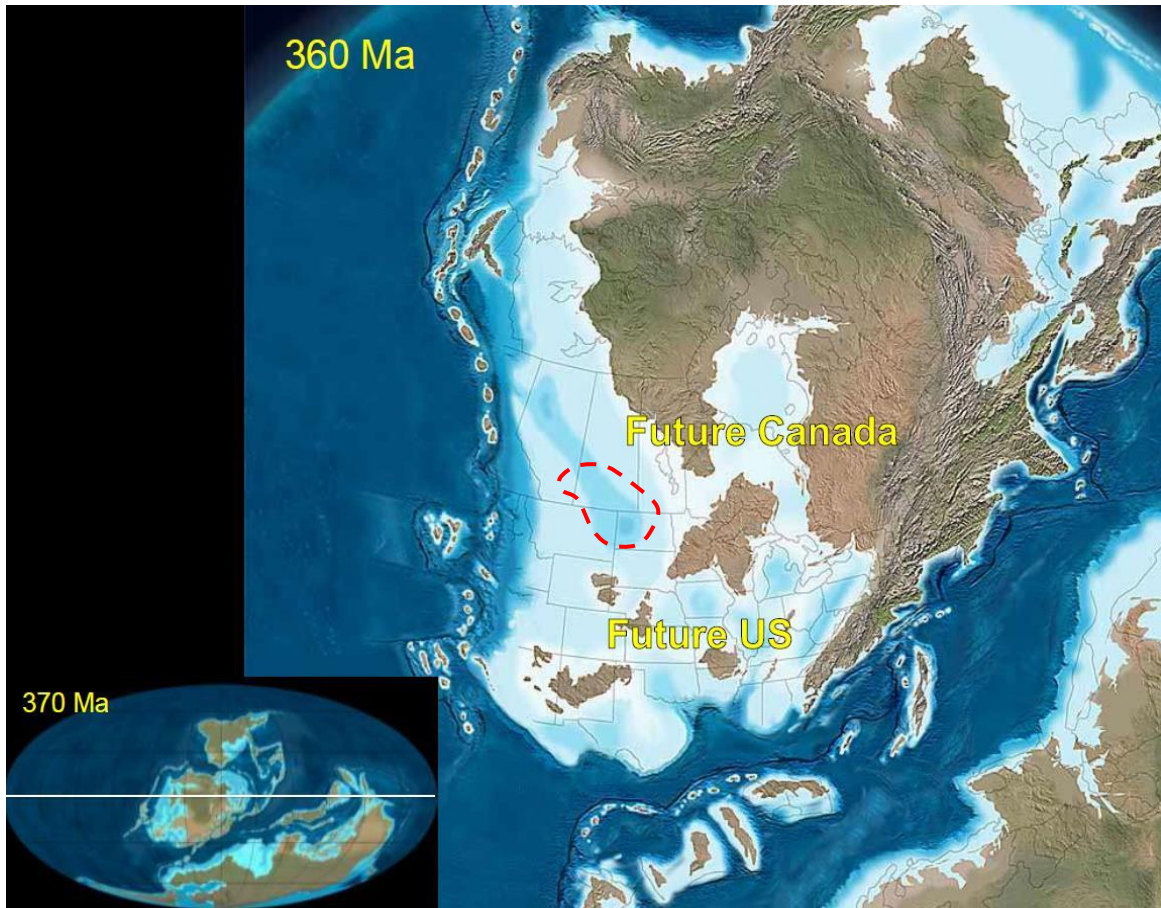


Figure 1.2: Reconstruction of North America in Late Devonian to Early Mississippian. Red outline represents estimated location of Williston Basin at this time. (Modified from Blakey, 2011)

1.2 Bakken Petroleum System Background

Oil generation, migration and accumulation of the Bakken Formation is summed up in Figure 1.3. As Pollastro et al. 2010 depicts in Figure 1.3, there are multiple phases of oil generation as the Bakken Formation was buried and the deeper extents of the formation enter the oil window.

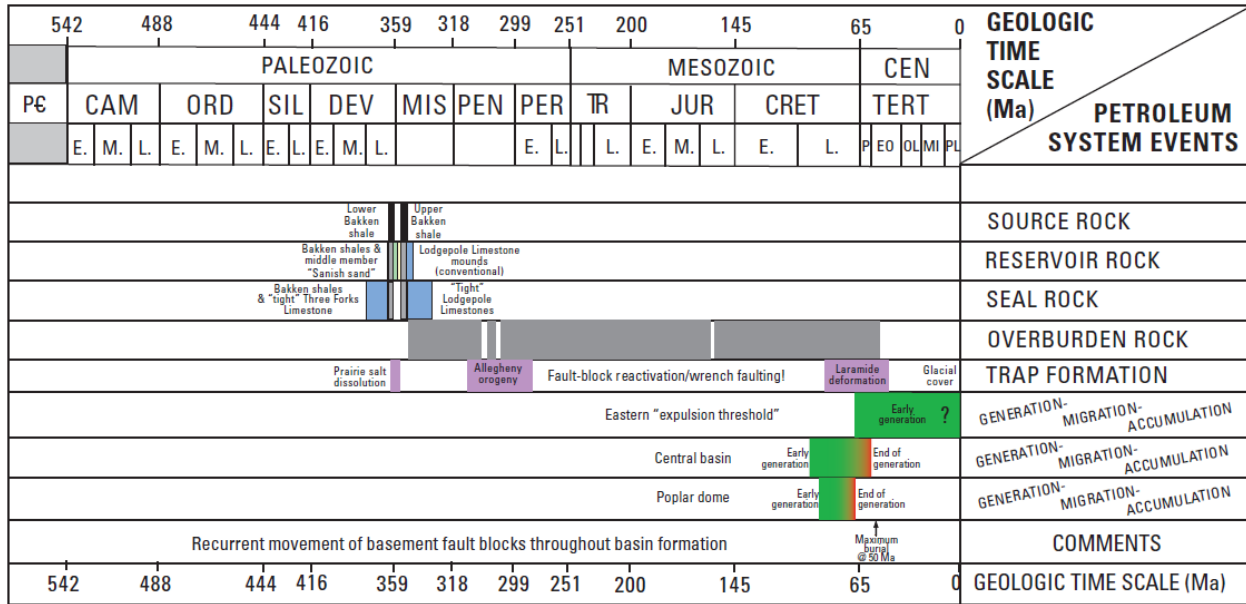


Figure 1.3: Oil bearing formation event timeline for the Bakken Formation (Pollastro et al., 2010)

In general, the Bakken had its source rock deposited during the Late Devonian (Lower Bakken Shale) and early Mississippian (Upper Bakken Shale). The reservoir rock, which is the Middle Bakken, was deposited in between the two source rocks. In addition, the seal rock is the source rock, but the zones of tight Lodgepole limestone or tight Three Forks limestone could act as a seal as well in the cases where the shale is fractured.

After the deposition of all the necessary petroleum system rock, they were sufficiently buried with overburden rock. This was then followed by the Allegheny orogeny and the Laramide orogeny, causing deformation and the development of anticline structures as seen in Figure 1.4. As seen Figure 1.2 previously, there was ample accommodation space for deposition above the Bakken, which created sufficient overburden. As you can see in Figure 1.5, Pollastro et al. 2010, burial curves of Bakken wells in North Dakota do not show oil generation until the Late Cretaceous following or during the deposition of the Pierre shale. Since oil generation occurred in the post trap formation phase (see Fig. 1.3), accumulations of oil is possible and is confirmed with the current oil production throughout the Williston Basin.

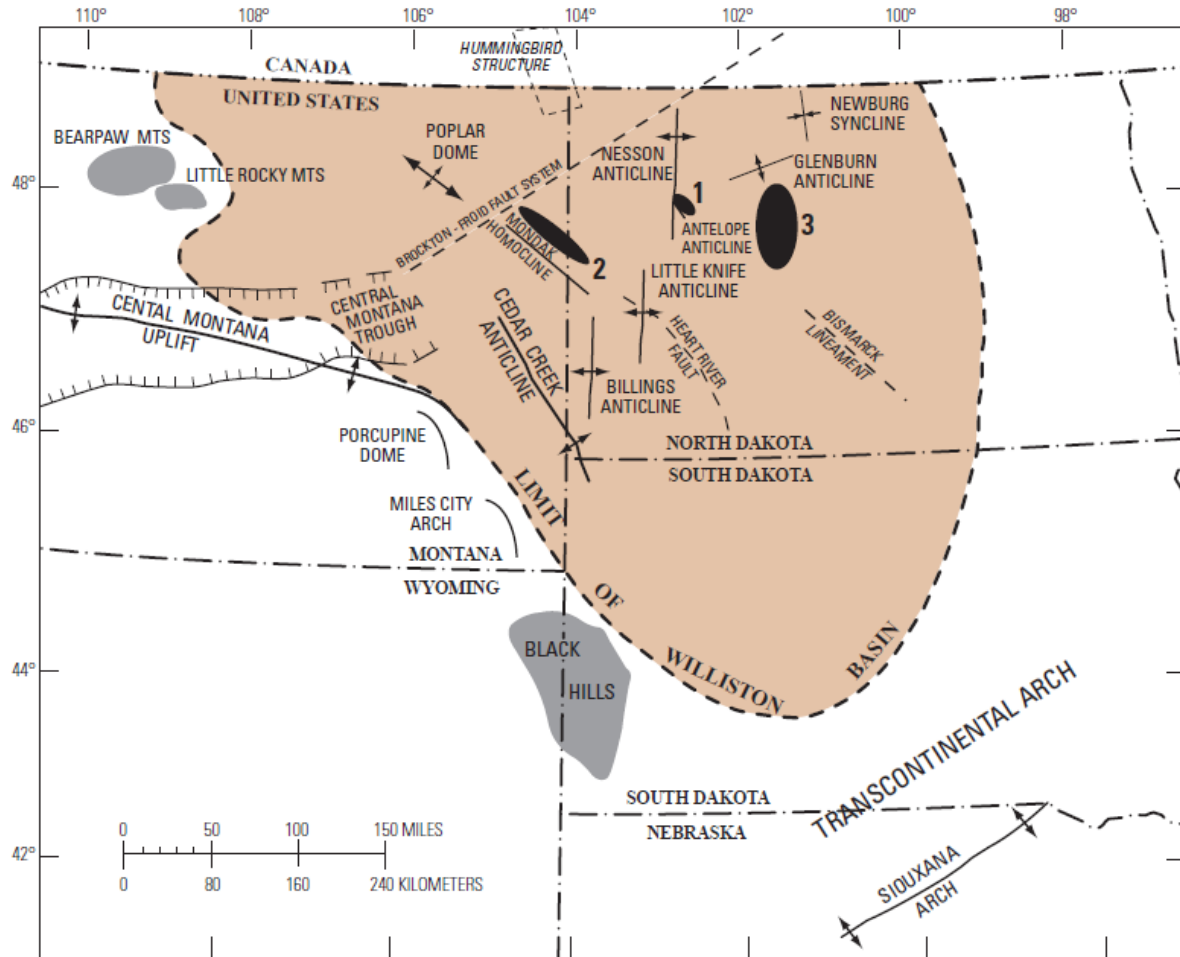


Figure 1.4: USA extent of the Bakken Formation. Depicts structural features from previous deformations. Solid black oval areas are general locations of oil production (1) Antelope field, (2) Elm Coulee Field, (3) Parshall and Sanish Field. (Pollastro et al, 2010)

Although the orogenic events did cause some anticline structure formations, the trapping mechanism of the Bakken is the reservoir rock itself. Generally, the oil expelled from the upper and lower shales were trapped into the low permeability of the Middle Bakken Member, the Three Forks Fm. and lower Lodgepole Fm. due to capillary pressures variations (Sonnenberg et al, 2009, Jin et al, 2013, and Wang et al. 2011, 2012, 2016).

With this stratigraphy, the Bakken is an ultra-tight rock formation, with the middle member porosity averaging about 5%, and permeability of about 0.04 md (Pitman et al., 2001). The source rock for the Bakken is the Lower and Upper Bakken Shale; the reservoir rock for the

Bakken is its middle member, Threeforks Fm. and lower Lodgepole Fm. However, for this research the focus will be on the middle member reservoir particularly the upper most portion consisting of dolostone with porosity of up to 2.5-8% porosity and permeability of 0.025-0.25 md (Sonnenberg et al, 2009). As a result, the Bakken is an ultra-tight system; the source rock expels the oil into the reservoir rock with very little migration. In addition, due to the extremely low permeability and high capillary pressure forces of the reservoir rock, the dolostone of the middle member also acts as a seal for the petroleum accumulation.

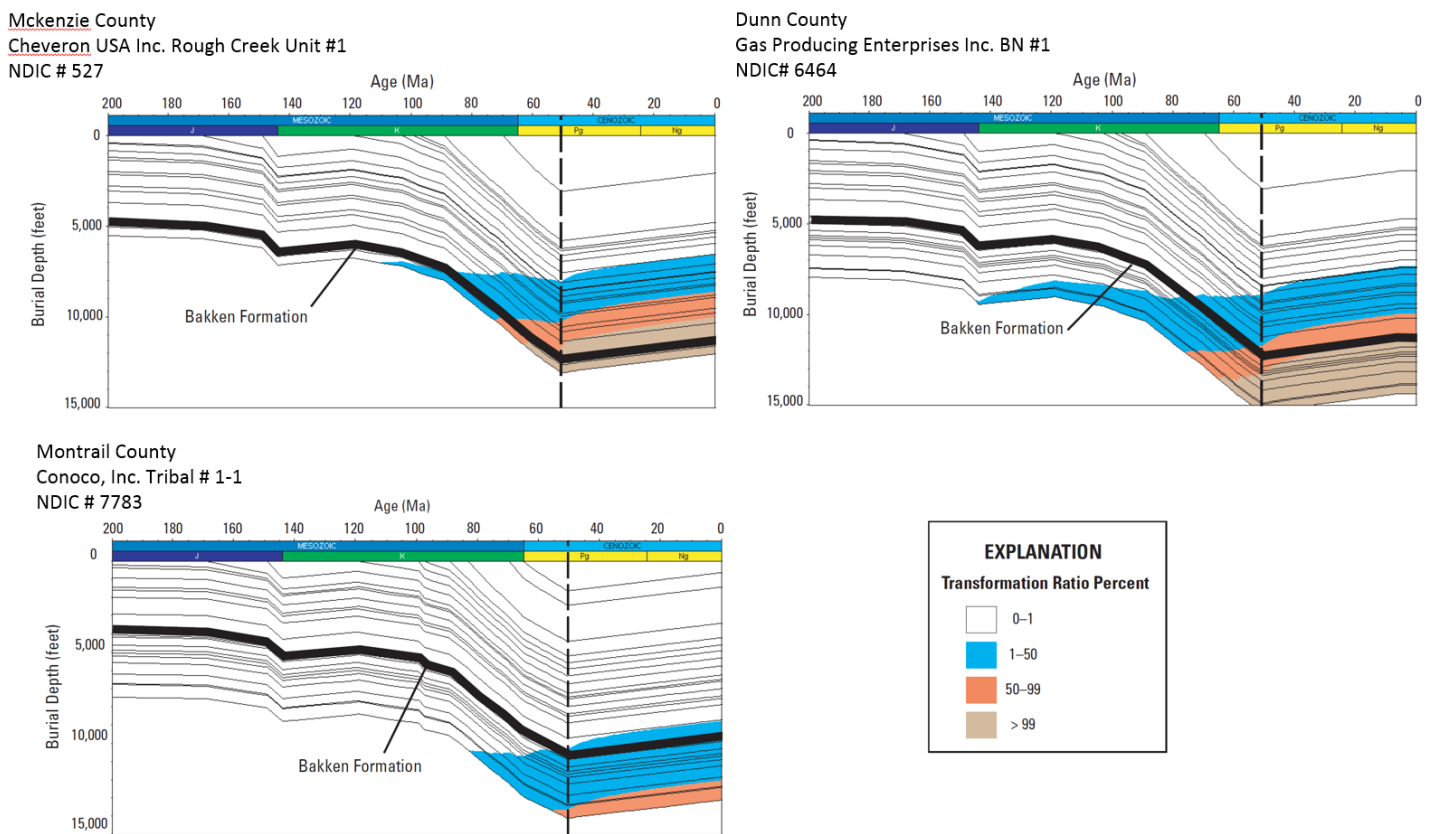


Figure 1.5: Burial history curve of three well locations in the Willison Basin North Dakota. Well names and file numbers located to top left of each curve set. Colors on burial curves represent calculated transformation ratios with respect to burial depth, time, and temperature. Bold line represent the Bakken Formation. Dashed line is the 50Ma age (modified from Pollastro et al. 2010).

1.3 Oil Recovery History of Bakken Wells and Proposed EOR Method

With the modern drilling techniques of today, there has been a massive increase in domestic oil production for the USA. The USGS estimates the reserves to be 7.38 billion barrels of

recoverable oil in the Bakken and Three Forks Fm. (Gaswirth et al., 2013). However, with nearly 12,000 wells producing from the Bakken (as of January 2018 DMR monthly reports) most are in the primary recovery stage, with a few running in the secondary recovery stage. Currently, it is estimated that the primary oil recovery factor (ORF) for the Bakken is to be less than 15% of the original oil in place (OOIP) (Yu et al, 2014).

In response to the Bakkens current ORF, lab work was done by Wang et al 2011, 2012, and 2016 with surfactant formulas and imbibition techniques that were hypothesized and tested. Surfactants are chemical solutions to alternate wettability and reduce the surface tension of water and the interfacial tension between liquids and solids. Surface tension is the ability for a liquid to stay attached to a solid particle by the internal forces between particles in the liquid (e.g. polar bonds between water molecules). Interfacial tension is the frictional tension forces between two different liquids or liquid and solids measured in force (milli-Neutons) per length of travel (meters) [mN/m]. By reducing surface tension and interfacial tension between liquids, immiscible liquids mix. This is one of the main reasons for focusing on surfactants; by having immiscible liquids mix we can change the wettability of the petroleum system. Wettability has three states in petroleum systems oil-wet, water-wet and mixed. Oil-wet systems have grains saturated with oil and pore spaces filled with a water/brine solution. Water-wet systems are the opposite with the grains saturated with water and the pore spaces occupied with oil. By changing wettability from oil-wet to water-wet, we can remove oil adhered to grains or held in place by capillary forces with water/brine and thus increasing the amount of recoverable oil trapped in low permeability, high capillary reservoirs (Wang et al, 2012).

There are many different types of surfactants, but most have the same basic construction; a hydrophilic head and hydrophobic tail. The hydrophobic end of the surfactant molecule is

designed to weaken the ionic forces water molecules have with each other which allow for water's strong surface tension. The hydrophilic head is present to make sure the surfactant compound is not expelled completely from the solution. As a result of the alteration of wettability from an oil-wet system to a water-wet system or the release of oil trapped via negative capillary forces, oils are able to move with less resistance in water, as the surfactant lowers the potential energy requirement for motion in water solution. These bundles of oil surrounded by surfactant mixed in water are usually denoted as micelles (Harwell, 1999).

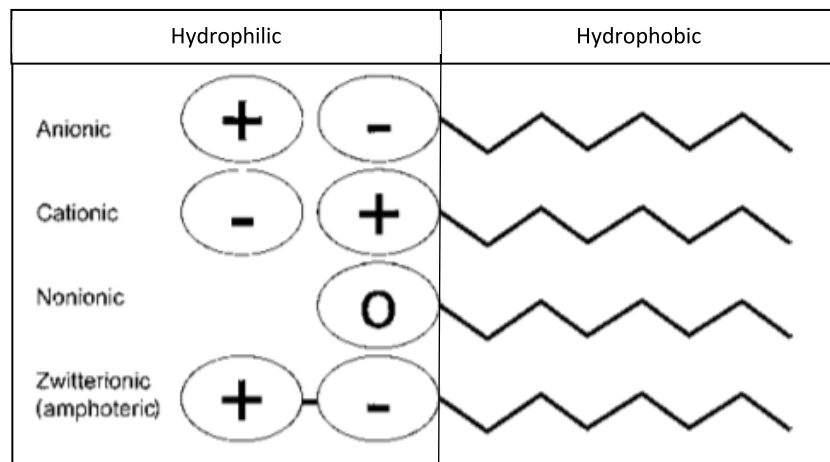


Figure 1.6: Top to bottom, Nonionic, Anionic, Cationic, and Amphoteric Surfactant molecules (Modified from Malmsten, 2002)

Surfactant types usually fall into four major categories: Nonionic, Anionic, Cationic, and Amphoteric as seen in Figure 1.6. The purpose of the different charged heads of the hydrophilic group is all dependent on which two immiscible liquids are interacting with each other, and how you want the surfactant to interact (Rosen et al., 2012). In simplistic terms, anion surfactants are used if the surfaces of the immiscible liquids boundary have a net positive charge. Cation surfactants are similar to anion surfactants, but used when the boundary surface has a net negative charge. Nonionic attaches onto the surfaces of the hydrophilic or the hydrophobic immiscible fluid boundary and orients towards that surface depending on the lowest potential energy orientation (Rosen et al. 2012). This makes nonionic very adaptable for multiple solutions

systems. Amphoteric is similar to nonionic as it can adapt to either immiscible fluid but as it adheres to the surface it does not change the charge of the boundary surface significantly (Rosen et al., 2012). Each surfactant group has its advantages in different applications.

Wang et al, 2012 used surfactants as a means to enhance oil recovery (EOR) by changing the wettability of samples in a lab setting. The study compared multiple methods of analysis for each surfactant type with various cores from the Williston Basin Bakken Formation. The conclusions from this study showed that with the addition of surfactant enhance oil recovery (EOR) could increase oil production between 6.8- 25.4% OOIP compared to brine water imbibition. The variation in oil recovery depends on the testing apparatus, initial condition and version of surfactant used. This conclusion is impressive as 1% OOIP increase of oil recovery could equate to about 100,000 bbls/month in the North Dakota oil field based on current production results as of January 2018 (DMR, 2018). Thus, if we use the surfactant results from Wang et al. 2012 in the basin at 6.8% OOIP increase we could possibly recover an additional 680,000 bbls/month at the lowest estimate based on the above assumptions. The next logical step would be to see if the Wang et al. 2012 research could scale up to field scale and produce a similar increase in barrels per month by using numerical simulation models.

Rai et al, 2013 attempted to simulate surfactant flooding in CMG-Stars model for a 20 md reservoir. He designed a model that could replicate lab results in computer simulation from core tests, thus showing that real world lab tests could be modeled in CMG-Stars. In the Romadhona et al, 2013 paper, they discuss the predictive modeling criteria for huff-n-puff injection of surfactant, similar to this paper's proposed enhance oil recovery (EOR) technique. Huff-n-puff or cyclic injection processes is a method of oil recovery that is designed to inject a solution or gas (e.g. Brine or CO₂) to re-mobilize the oil and to increase production. In Romadhona et al, 2013

they show that surfactant EOR simulation can be modeled in CMG-STARS and that accuracy in predicative quality depends on the modeling parameters of the model. Their paper also suggest that for successful surfactant EOR, interfacial tension (IFT) should be lowered to 0.07 mN/m, and that surfactant concentrations of 0.1- 2% for reservoir permeability's should be 20 md or lower. They also noted that for tight reservoirs, simulations and real-world huff and puff need to have an injection time and soaking period before production.

The inspiration for this research is a combination of Rai et al, 2013, Romadhona et al, 2013, and Wang et al., 2016 ideas but with the construction of a digital geological model. This research is to see if modeling the Bakken Fm. in CMG-Stars using lab data on surfactant EOR with permeability of 0.1 md and lower, rather than the 20 md used by Romadhona et al, 2013, can generate similar positive results found in Wang et al. 2012. In Wang et al. 2012, ORF values have been shown to be near 20% OOIP in Bakken Formation samples using ethoxylate nonionic surfactant of concentration of 0.05-0.1% in a salinity solution of 4-10 % TDS and formation salinity of 30% TDS (Total Dissolved Solids). The purpose of this research is to discuss a new methodology for geological evaluation and modelling that combines laboratory surfactant imbibition data, mapping software, a well log interpretation program & geological modeling three-dimensional (3D) software, and a functional reservoir numerical simulator to scale the surfactant lab results from Wang et al, 2012 to a real world scenario.

Success for this simulation will be measured on the following criteria:

- 1) Is the well production history match by the numerical simulation model in agreement with the actual production history? With this question, a relative error of the well production simulation vs. the real-world production history of less than 7% was used in this research as the threshold for a successful match. This criterion is based on the

Western Atlas Nolan Co. Black Oil numerical simulation manual of 1985, stating that a model with poor correlation to the real world production data is not a good simulation.

- 2) Does the generated Geological model and numerical simulation exist within real world parameters? If the parameters used in the model to calibrate production history match do not coincide with real world possibilities then the simulation fails for being unrealistic.

If these two criteria are satisfied, the simulation model will be considered a success in scaling of lab data to a field scale. If any of these criteria are not met, the simulation will conclude surfactant EOR simulation as ineffective or an error within the geological model.

1.4 Hypothesis

It is possible to successfully upscale the lab results from Wang et al. 2012 by simulating the production history of one well in the Bakken formation and get close to ORF values of 6-20% OOIP from the simulated surfactant imbibition process.

CHAPTER II

Methodology

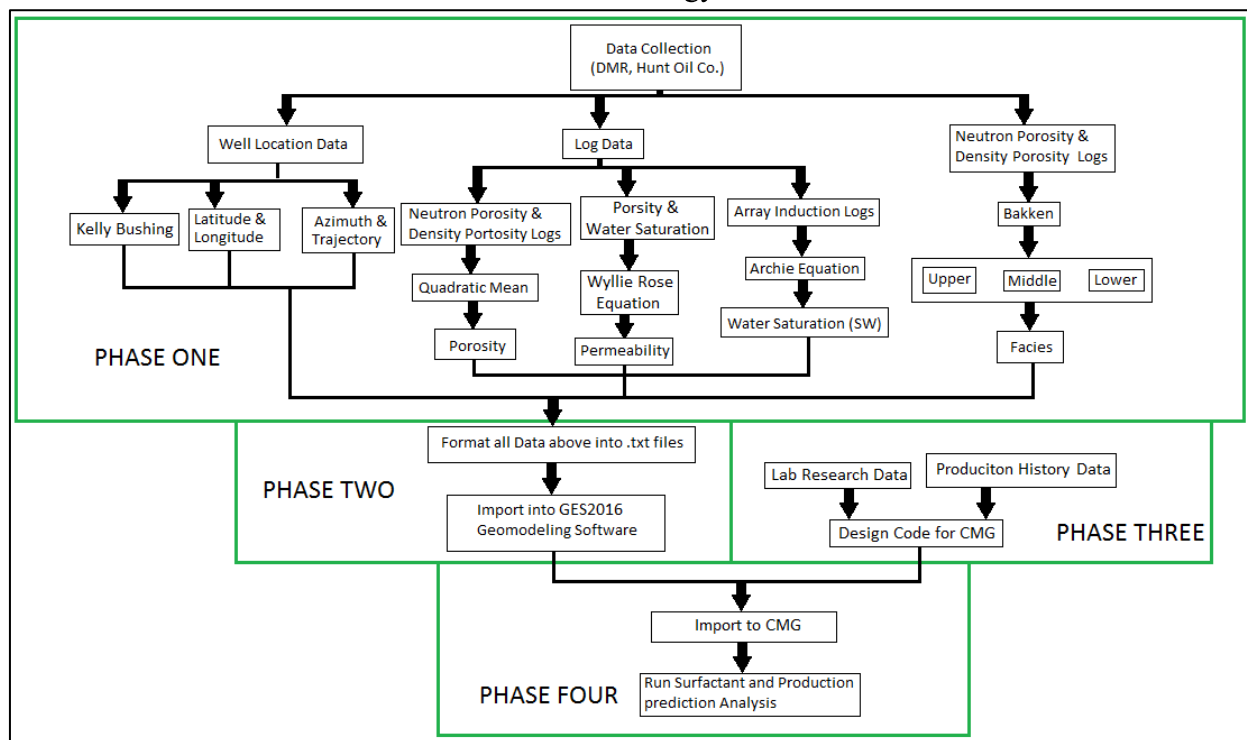


Figure 2.1: Initial workflow of how to construct a geological model and oil reservoir simulation model.

The procedure for modeling and simulating the Bakken Formation was done in four phases, Figure 2.1. Phase one – well selection and data collection done via ArcGIS and North Dakota Department of Mineral Resources Oil and Gas Division website. Phase two – geological model construction using Geologic Evaluation Software 2016 (GES2016) from Golden Sun Petroleum Technologies (GPT). Phase three – calibration of simulation of the geologic model and an isolated well using Computer Modeling Groups (CMG) Builder and STARS modeler programs. Phase four – forecasting and comparison of surfactant injection trial in CMG simulation and analysis of accuracy of simulation.

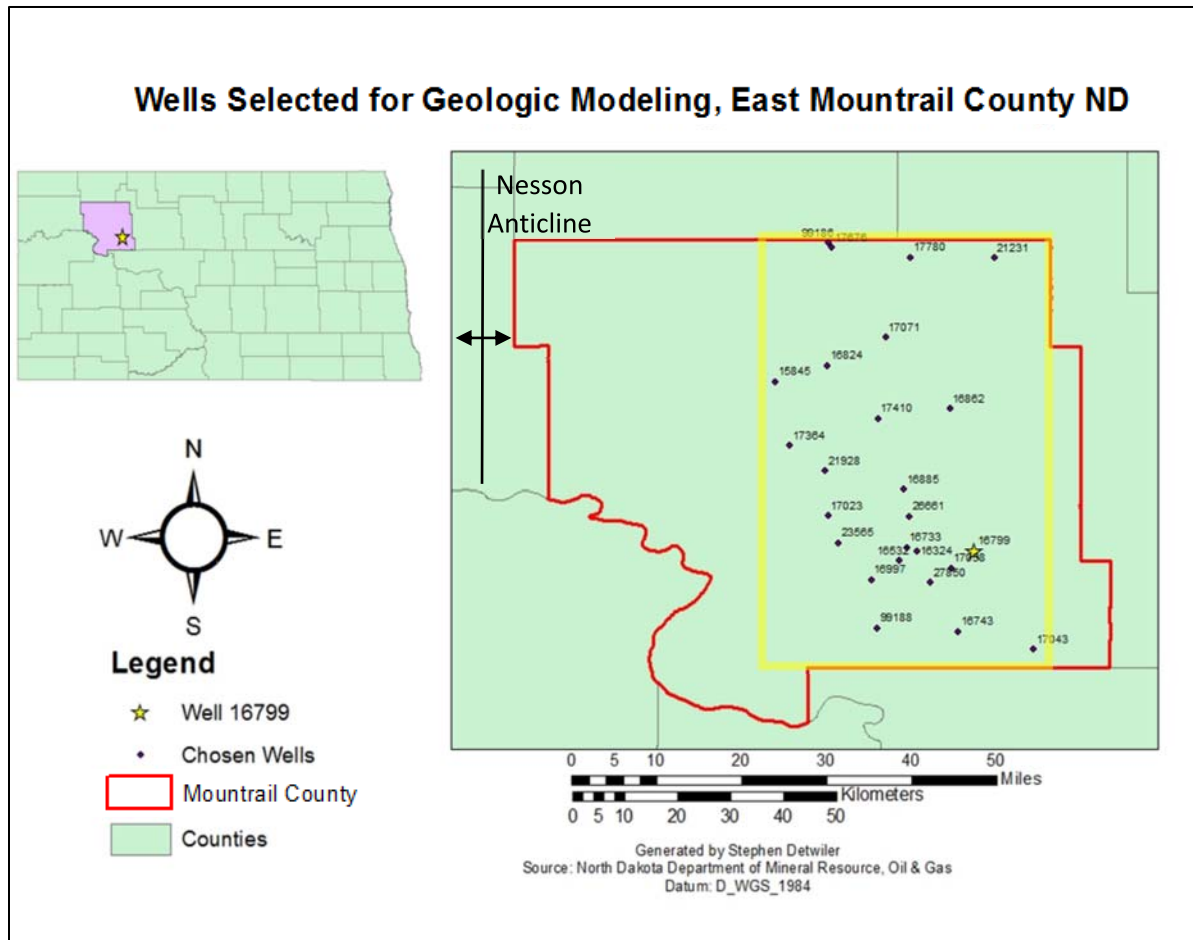


Figure 2.2: Map of Mountrail County with the 24 wells used for 3D modeling. Yellow highlighted area is the extent of the area that will be 3D modeled

Phase 1: Data collection and filtering

Figure 2.2 is the map for the extent of the geological reservoir modeling area the wells selected for modeling. The highlighted well is for the surfactant EOR effectiveness simulation. The basis of all field data acquired comes from the public database of the North Dakota Department of Mineral Resources (DMR) Oil and Gas Division website (DMR, 2018). Starting with the database of over 3000 wells in shapefile format, the wells were imported along with a table file of all recorded logs for each well; both were provided by the DMR database. In ArcGIS, both the well locations and full log dataset were displayed and related based on API

numbers. Mountrail County was chosen due to its close proximity to the Nesson Anticline and for the large number of recent wells that would likely have more digitized wire log data. Parshall Field in particular was looked into further because of it being near the edge of the Bakken maturation boundary, thus making it an area of key intrigue (Lefever, 2008). The selection criteria to filter the wells of interest need to include: Array induction logs (AIG), Compensated Neutron Density logs (CND), formation top records for the Bakken & Three Forks Formations, and to be located on the Eastern half on Mountrail County.

Array induction logs are electrical resistivity measurements. AIG's are a long sonde device with a transmitter at the bottom and receiver at the top (Selley et al, 2015). The transmitter generates a magnetic field, which creates an electrical current in the formation. This electrical current is then picked up by the receiver at the other end of the sonde. The magnetic field is then adjusted for different ranges of distance into the formation from one to four feet. The reason AIG logs are necessary data for a well to have for modeling was its relationship to porosity and fluid saturation in the formation. AIG logs show how resistive a formation is to electrical current, brine is very low resistivity compared to both oil and rock which are highly resistive.

Compensated Neutron density logs are a suite of a few different radioactive sonde measurements. The few of importance for this project are Neutron Porosity log (NPOR), Density Porosity log (DPHZ) and Gamma Ray log (GR). The GR logs are a simple measurement of radiation emitted from the formation, usually due to radioactive Potassium (K), Thorium (Th), and/or Uranium (U) (Selley et al. 2015). Neutron porosity logs are a sonde device that bombards a formation with neutrons from a radioactive source (Selley et al, 2015). This causes the formation to emit gamma rays proportional to the amount of hydrogen atoms present in the

material. Thus, since oil and water have a very large concentration of hydrogen atoms (compared to rock) they display a signal that can be interpreted as porosity. Compensated density logs is a similar well-logging method to NPOR. However, the DPHZ emits gamma radiation and with the return signal giving us a bulk density (Selley et al, 2015). This signal is corrected based on properties of the well. The corrected data is correlated to the density of lithology of a dry sample of the formation and to the density of the fluid in formation. This calculates the porosity signal for the formation as well.

Wells were selected for this research based on the presence of the necessary logs (CND suite and AIG suite), formation tops (Bakken and Three forks Tops from DMR database) and location (east Mountrail county) and was accomplished by using ArcGIS 10.4's definition query. ArcGIS is a software suited for picking wells of interests because of its ability to preserve all meta data of each single well, but also allows filtering options via the meta data and spatial relationships. The criteria for the well selection was done in this way to make sure that all wells selected have a relatively straight pilot hole that penetrates through the entire Bakken Formation. The straight pilot hole is necessary for modeling the Geophysical properties in Phase 2 in the geological modeling software. The outcome of the ArcGIS utilization in the target formation of this research produced 24 wells for geological modeling as seen in Figure 2.2 and full detail of each well seen in Appendix C.

Phase 2: Geologic Modeling

After the wells were identified with ArcGIS, the appropriate digital (.las) files were downloaded from the DMR website and imported into excel for analysis and simplifying. The data for each well was verified compared to the drill time - mud log records for each well to adjust for depth discrepancy between logs. For the CND logs, measured depth, Neutron Porosity

(NPOR), Density Porosity (DPHZ), and Gamma Ray (GR) logs were isolated and exported as text files for importing. For the well trajectory data, measured depth, azimuth, and inclination data were all imported into excel and exported as a text file. In addition, the trajectory data was edited by removing paths that were not logged by the CND and AIG sondes. This included most of the laterals and side tracks of the selected wells, except well file #16799. AIG logs were imported into excel, and then the two-foot and four-foot induction suites were averaged as a Resistivity of formation (R_t) value (Doveton, 1999 and Crain, 2015). Lastly, the well ID, latitude, longitude, and Kelly Bushing elevation (elevation of the top of the well, beginning of measure depth values) were compiled from the DMR database into one excel document and exported to a text file.

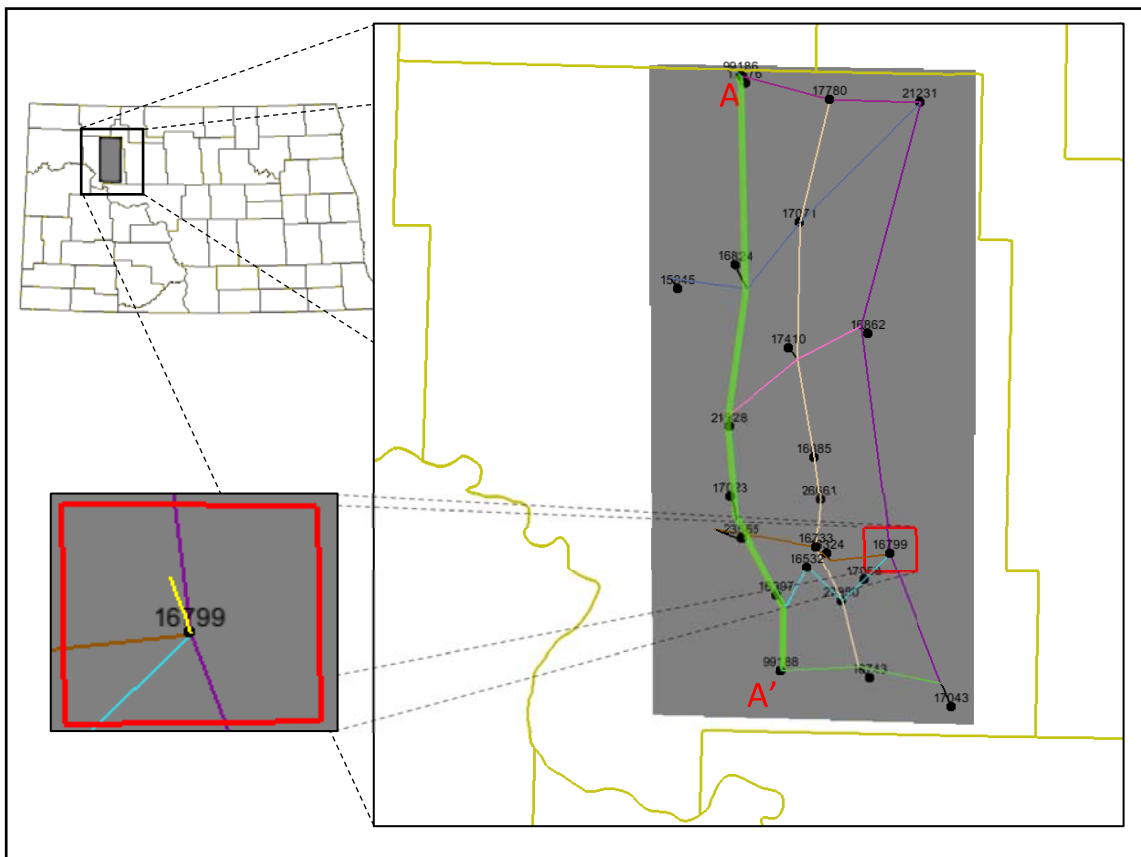


Figure 2.3: Map of North Dakota and the modeled area used in Geological modeling- GES2016. Area comprises of Eastern half of Mountrial County, There are a total of 24 wells and nine Cross sections made for well correlations. The red highlighted area is the extent of the model used in numerical simulation - CMG-STARs, and shows trajectory of well # 16799.

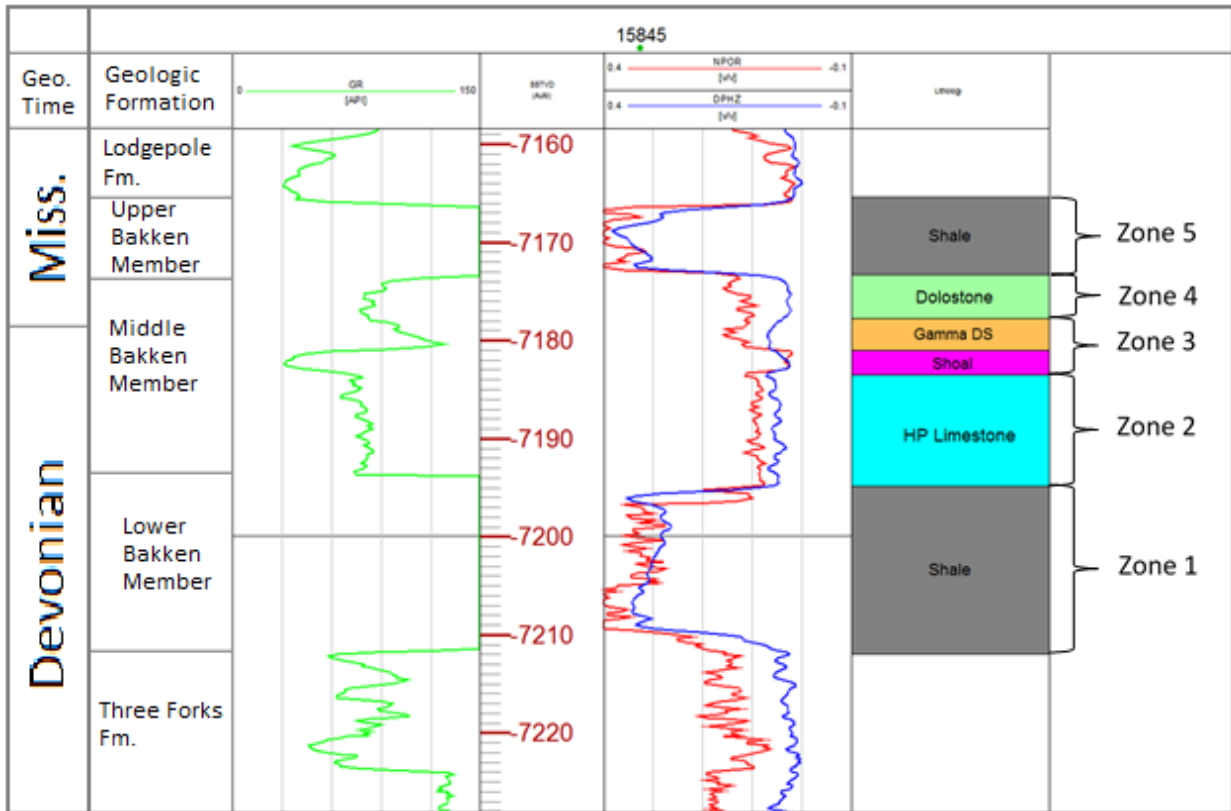


Figure 2.4: Reference Section of well #15845. Section includes Petrophysical data (Starting left to right) on Gamma ray signature, SSTVD Depth in feet, NPOR and DPHZ signatures, and Lithology classification based on Petrophysical Data. Zones were established based on reoccurring patterns seen in all wells from cross section correlations

All above compiled data was imported into the geological modeling software GES2016 along with North Dakota county shapefiles. GES2016 was used as the 3D modeler because of its ability to correlate well cross sections, spatial tool analysis, efficient petrophysical analysis and intuitive interface for 3D modeling. The reference datum used for projection of the spatial data of the model was North American Datum of 1983 (NAD83). Once imported, the data was displayed in 2D map view format to create cross sections for well correlation. A total of three north-south cross sections and six east-west cross sections were created as the Figure 2.3 shown. Each cross section correlates the gamma ray, neutron porosity, and density porosity logs for well to well cross section. The CND suite of log data allows us to pick lithological differences in the data with relation to depth and signal values allowing for subsurface correlations without rock core

observation for each individual well. Consequently, five zones of petrophysical facies were created: the Upper Bakken Shale, upper-Middle Bakken, central-Middle Bakken, lower-Middle Bakken, and the Lower Bakken Shale. Using the geophysical properties and the lithologies; zones were established based on log patterns and value ranges (Figure 2.4). Figure 2.4 shows the reference section of layers established by petrophysical properties. To verify the geophysical signals correlation with rock, a comparison between the lithology and log patterns was completed with a log of the Well #15845 and core samples provided by the UND Core Library. Once correlations were established, the effective porosity log was calculated by a square root average (see equation 1) [Asquith et al., 1982, Crain, 2015, Doveton, 1999, Simenson et al., 2013]. Water saturation was calculated using the Archie equation (2) [Asquith et al., 1982, Crain, 2015, Doveton, 1999, Simenson et al., 2013]. In addition, the permeability was calculated with the Wyllie Rose equation (3) [Asquith et al., 1982, Crain, 2015, Doveton, 1999, Simenson et al., 2013]. See nomenclature section on page 41 for variable definitions for all equations. Log-Core calibration equations would be a better calibration for calculating these properties. However with the simplified equations presented earlier, they were calibrated via comparison to core lab analysis samples done by the companies owning the wells for porosity, permeability, and water saturation. The outcomes of the lab results were then compared to outputs from the equations, and the variables of the equations were adjusted accordingly to fit the lab data (See Digital archive for Lab-core sample outputs). These three equations were computed for all wells. Upon completion, the GES2016 “one-button” function was utilized to construct the final 3D model, see Table 2.1 for parameter settings used.

$$\phi_e = \sqrt{\frac{(\phi_D^2 + \phi_N^2)}{2}} \dots\dots\dots \text{Equation (1)}$$

$$S_w = \frac{n \sqrt{\frac{a * R_w}{\phi_e^m * R_t}}}{\dots\dots\dots} \text{Equation (2)}$$

$$K = C * \frac{\phi_e^D}{S_w^E} \dots\dots\dots \text{Equation (3)}$$

Table 2.1: Parameters for generating the 3D model in GES2016 of east Mountrail County, ND

Parameter	Description	Value
Grid Cell size (x,y)	Cell size in feet for each cell	500 ft
Number of cells z-dir (Zone 1,2,3, 4, and 5)	The number of cells given for each zone in z-direction	1 cell, 6 cells, 6 cells, 6 cells, 1 cell
Facies Log	Discrete data used for modeling and distinction of block wells	Lithology from Well correlation
Method Facies modeling	Equation for interpolating to unknown cells based on block wells	Sequential indicator simulation
Petrophysics Modeling method	Equation for interpolating to unknown cells based on block wells	Sequential Gaussian Equation
Water Saturation Block well Algorithm	Well site location to determine value of individual cells in intersects	Arithmetic Average
Permeability Block Well Algorithm	Well site location to determine value of individual cells in intersects	Harmonic Average
Porosity Block well algorithm	Well site location to determine value of individual cells in intersects	Arithmetic Average
Porosity Input Data	From calculated values for each individual well, normalized on histogram	Square Root Mean of Neutron and Density porosity logs
Permeability Input Data	From calculated values for each individual well, normalized on histogram	Wyllie Rose equation output values (Corrected for Shales)
Water Saturation Input Data	From calculated values for each individual well, normalized on histogram	Archie Equation Output values

Phase 3: Production History Matching

With the completion of the geologic model, the outcome file was exported and then imported into the pre-data processing module - reservoir numerical simulation software - CMG

Builder for conversion. CMG Builder is another program in the CMG suite. The purpose of the CMG Builder utilization was to format the data output from GES2016 to be usable for CMG STARS (the simulation software from the CMG Suite). As long as the data was exported from GES2016 in a binary rescue file format, the integrity and separation of the cell data generated from GES2016 will carry over to CMG-Builder.

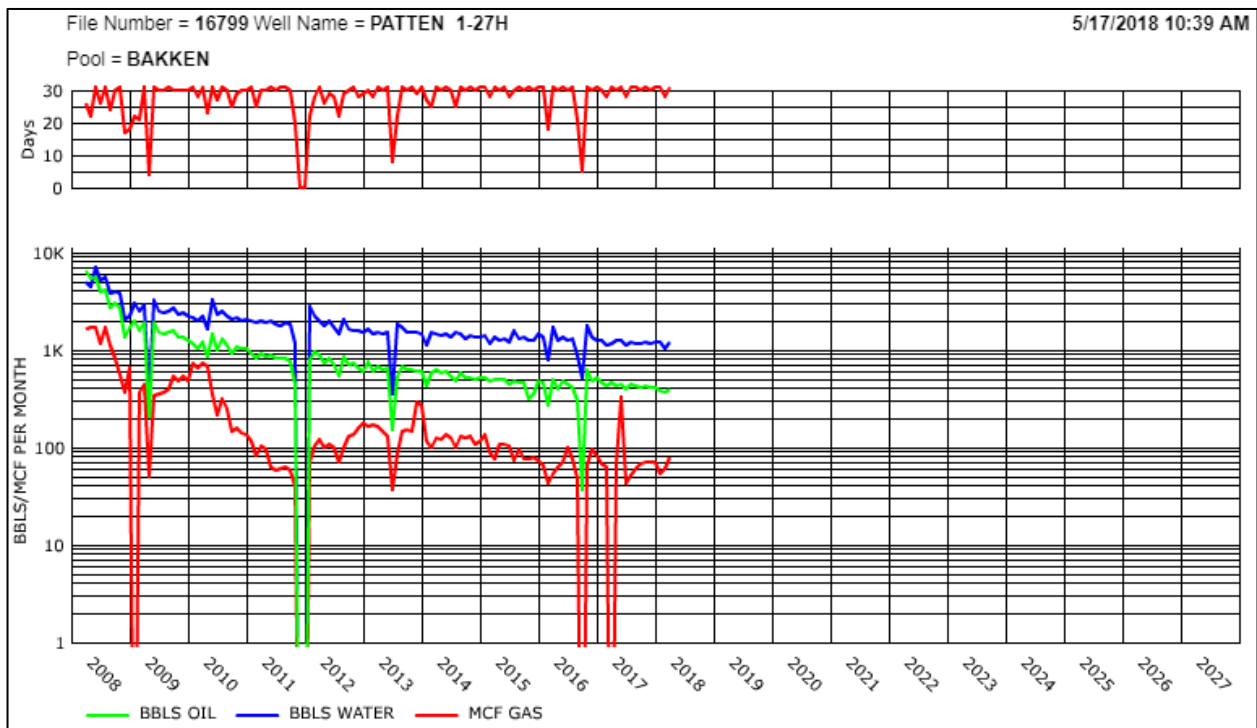


Figure 2.5: Production history of Patten 1-27H Well # 16799. Data provided from North Dakota DMR website (DMR, 2018).

At this point, the Well #16799 was selected as the well of interest for testing production and history matching. The well is located in Parshall field, and it operated by the Hunt Oil Company. Figure 2.5 shows the status of production for Well #16799 whose production data (provided by Hunt Oil Co.) we will be using to match to our simulation. Therefore, the full well trajectory of Well #16799 was imported into CMG builder as well. The numerical simulation model was trimmed down to a 20 x 20 x 20 cell area (See Table 2.1 for Cell dimensions)

surrounding the Well #16799, along with all geological and reservoir properties for each cell. Table 2.2 provides the petrophysical properties used to run the simulations for Well #16799 at the Bakken initial conditions (Wang et al, 2011, Nordeng et al, 2010). Correction for porosity of the upper and lower Bakken Shales were done in CMG post geologic modeling. History matching of oil production and water cut percentage was completed through relative permeability curve and other parameters (for example, initial formation pressure, etc.). The purpose of matching to known history data is to make sure the model produces the same results as real world production, which then allows for the possibility of forecasting future production. If calibration settings of the simulation curve need to exceed possible real world conditions in order to match the known production history, then the simulation fails as stated in the criteria for successful hypothesis. Calibrations were done in small increments to fit simulation production to real world production. It is implied that the adjusted values are not true to the formation, however due to the need to homogenize the data for cells covering a large area for simulation this is acceptable. On the other hand, Bottom hole pressure (BHP) was also used to calibrate the production history of Well # 16799, using equation (4) provided by Hunt Oil. By making sure the BHP is close to the actual conditions just gives another boundary line of constraint for the model which will make it more realistic.

$$BHP = \text{Casing pressure} + (0.3 * (TVD - \text{Fluid Level})) \dots\dots \text{Equation (4)}$$

Table 2.2: Averages of values generated for geological model and numerical simulation

Petrophysical Property	Average	Standard Deviation
Porosity Upper Shale (%)*	3.39	1.06
Porosity Middle Bakken (%)	8.1	2
Porosity Lower Shale (%)*	3.42	0.86
Permeability Upper Shale (md)	0.026	0.551
Permeability Middle Bakken (md)	2.46	37.82
Permeability Lower Shale (md)	0.039	2.3
Thickness of Bakken (ft.)	85.71	4.407
Water Saturation Middle Bakken (%)	28.6	20.7
Initial Reservoir pressure (psi)**	6000	-
Initial Reservoir salinity (%)**	30	-
Initial Reservoir temp (°C)**	115	-
Porosity Fracture (%)**	10	-
Permeability Fracture (md)***	0.01	-
Depth Upper Bakken Top (ft)	9204.78	405.95
Depth Middle Bakken Top (ft)	9213.80	446.75
Depth Lower Bakken Top (ft)	9351.81	416.02

(*)= Calibration was done in CMG post Geological modeling based on Ramakrishna et al., 2010 and core lab test seen in digital archive.

(**) = Single input to model via research investigation Wang et al, 2012 and Nordeng et al. 2010.

(***) = Used minimum value for possible permeability fracturing, Wang et al, 2012.

Phase 4: Surfactant Imbibition and Effectiveness Forecasting

Surfactant imbibition properties were added after post production history dates, and all subsequent calculations only affect imbibition process. The nonionic surfactant formulation seen in Wang et al. 2011 was used for the surfactant imbibition forecasting. Surfactant concentrations of interest were 0.1%, 0.5%, and 1.0% to scale with Wang et al. 2011. Trials for the length of the imbibition process were evaluated as well, regarding to length of time for injection, soak time, and production time, similar to the considerations done in Romadhona et al., 2013. This was completed by a cyclical pattern, huff-n-puff, over a 10-year period to allow for visual contrast between trials. Lastly, sensitivity analysis was performed with a $\pm 20\%$, $\pm 10\%$ adjustment to each physical property setting for investigation of the importance of each variable.

CHAPTER III

Results

Figure 3.1 shows the initial results from ArcGIS of a simplified contour structure of the Bakken Formation in Eastern Mountrail County. This was completed as a verification to ensure that the 3D model generated from the geological modelling was accurate.

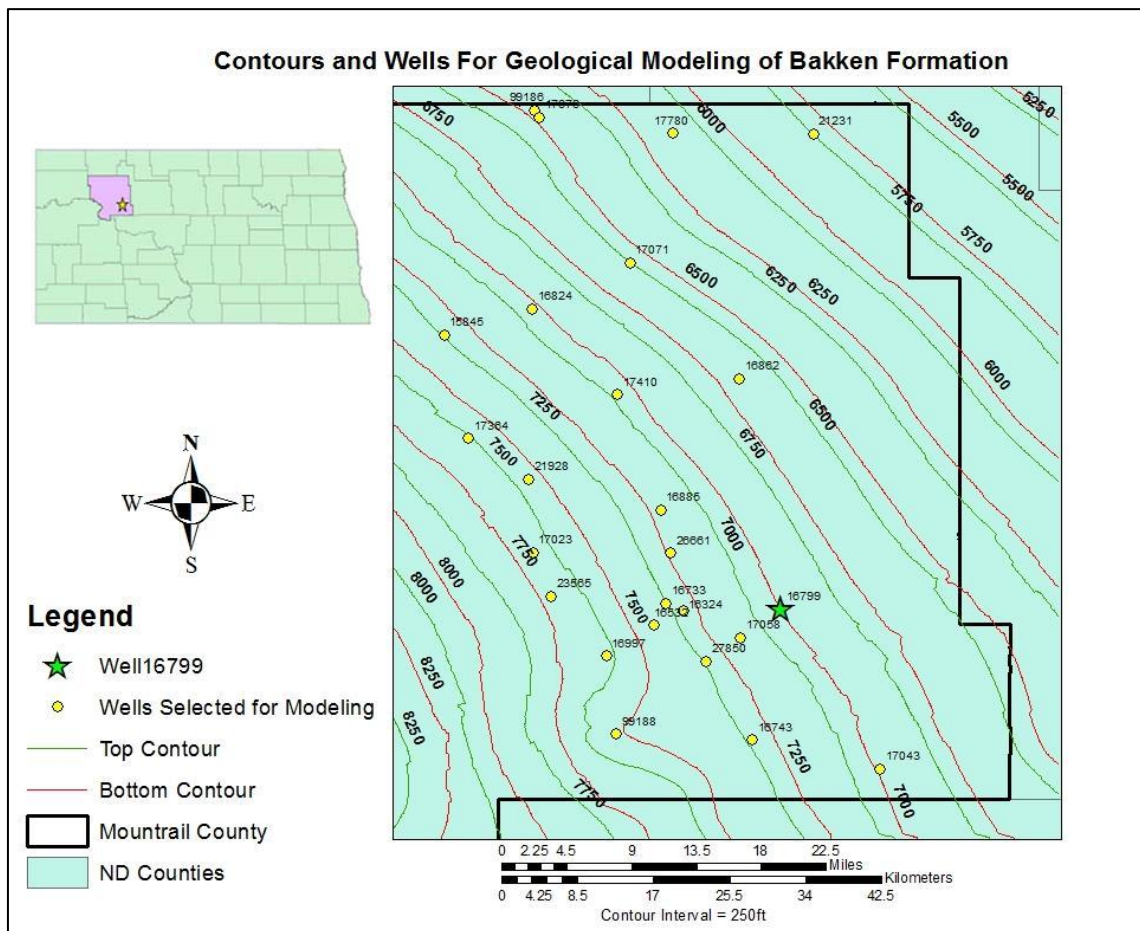


Figure 3.1: Contour map of Eastern Mountrail County generated in ArcGIS from 610 wells within and surrounding Mountrail County. Datum used was NAD27 and contour values are elevations below mean sea level. Tops were selected and corrected from Kelly Bushings readings from data provided by DMR, 2018. Constructed with Empirical Bayesian Kriging (EBK). Top contour represents the top of the Bakken Fm., bottom contour represents the top of the Three Forks Fm. Highlighted wells represent the 24 wells with necessary petrophysical data used for geologic modeling.

The variables for equations 2-4 are shown in Table 3.1 and were used to generate all the values needed in GES2016. Constant values for the Archie and Wyllie Rose equations were derived from a compilation of previous works around the Bakken [Crain, 2015, Doveton, 1999, Simenson et al., 2013, Schlumberger, 2009]. The Archie equations value choices were derived from the work of Simenson et al. who generated tortuosity component (a), saturation exponent (n) and cementation exponent (m) variables seen in Table 3.1 from their research on the Bakken Formation by facies in Core sample analysis (Simenson et al., 2013). The formation water resistivity (R_w) was generated from the lab work of Wang et al., 2011, 2012, and 2016 on formation water solution composition and formation temperature. Using Wang et al. 2011, 2012 and 2016 as the source formation temperature and salinity, these values were used in Schlumberger, 2009 resistivity chart to find the values of R_w . Wyllie Rose equation variable were generated from Crain, 2015. Hunt oil TVD value was selected based on the average elevation of the trajectory of Well #16799. All the aforementioned equations also had adjustments to variable input based on correlation to state well records generated porosity, permeability and water saturation (see digital archive).

Table 3.1: shows equations (2-4) constant values used for log data calculations and cell value generation.

Equation	Variable	Value
Archie	a	1
Archie	n	1.74
Archie	m	1.62
Archie	R_w	0.02
Wyllie Rose	C	62500*
Wyllie Rose	D	6
Wyllie Rose	E	2
Hunt Oil BHP	TVD	9050 ft

(*)= Upper and Lower Bakken shales used 6250 for C in Wyllie Rose calculation

Table 3.2 shows the Bottom hole pressure calculations with equation (4). Bolded values are the ones used in the numerical simulation, where the others are from the raw Hunt Oil production

data. Note there is an increase in pressure as time increase for initial simulation, however it does stabilize close to Hunt Oil’s BHP data.

Table 3.2: represents bottom hole pressure from Hunt Oil Co. data and equation 4, Bolded values are the BHP needed to history match to production data.

Time (Days from production start)	BHP (psi)
730	1700
1460	2200
2150	2472
2190	2850
2420	2739.5
2690	2738.4
2920	3000
3170	2765

Figure 3.2 depicts a single structural well correlation from one of the nine cross-sectional correlations, as seen in Figure 2.3 with the Green highlighted cross section A-A’, made in GES2016 to create the 3D model.

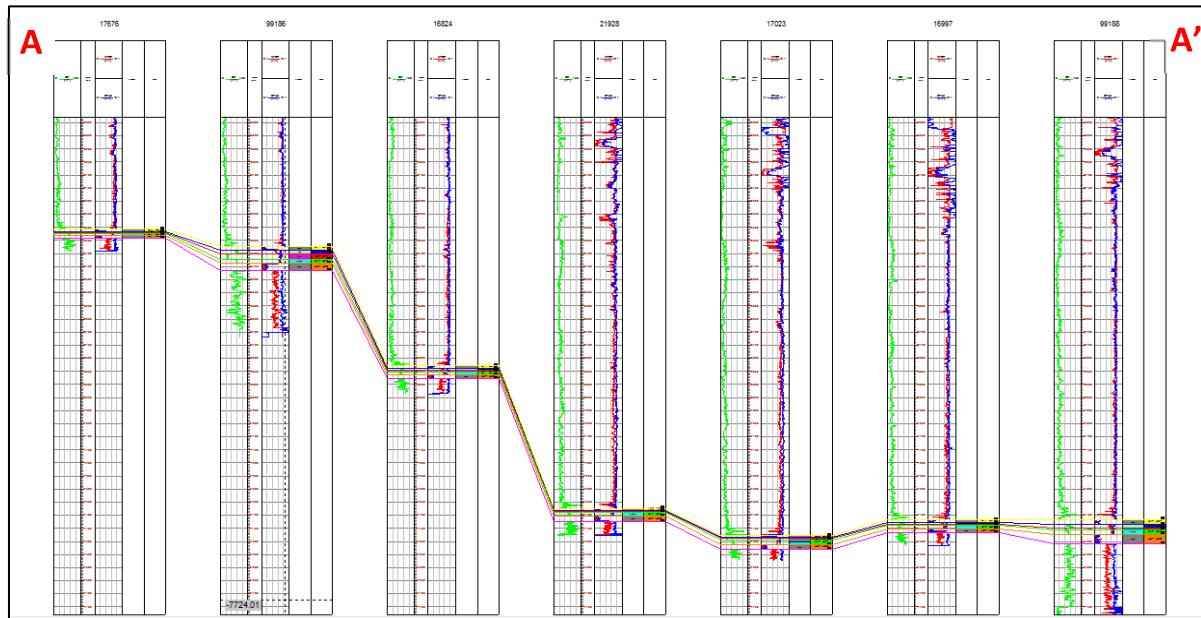
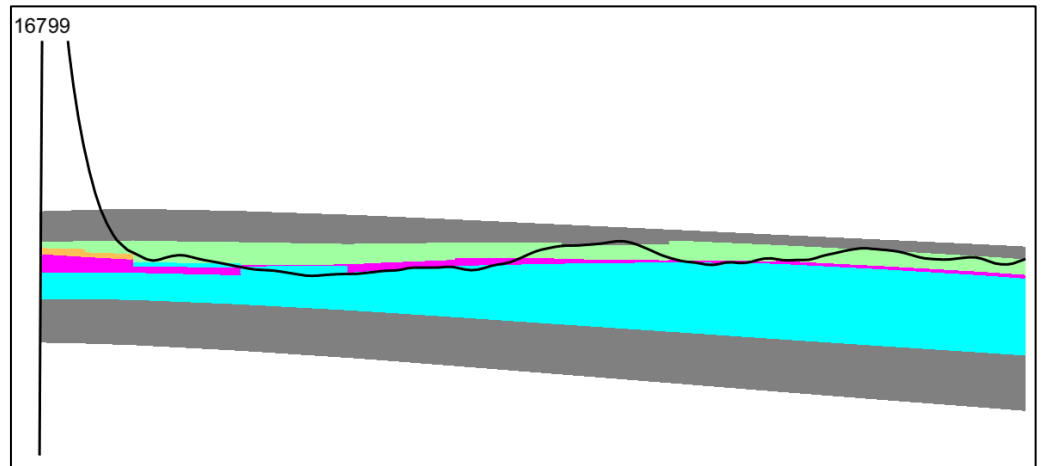


Figure 3.2: Structural well correlation of (from left to right) wells # 17676, 99186, 16824, 21928, 16997, 99188. Cross section matches with A-A’ cross section seen in Figure 2.3.

Figure 3.3 depicts a 2D lithofacies cross section along the trajectory of Well #16799. The map view trajectory can be seen in Figure 2.3. This trajectory was fit to the model based on the

Drill time –samples- Mud log (DTSM) data provided by DMR, 2018 (see digital archive for full DTSM file).

Figure 3.3: Cross Section along the trajectory of Well #16799. Cross section represents the lithofacies. Grey = Shale, Green = Dolostone, Blue = Limestone, Pink = Shoal, Orange = Gamma High Dolostone. Vertical trajectory is the pilot trajectory used for modeling, Horizontal trajectory was used for Contour correcting.



Comparison with Well #15845's core and logging data as seen in Figure. 3.4. Log data was divided into 5 zones from bottom to top of petrophysical facies: Zone 1 - the Lower Bakken Shale, Zone 2 – lower-Middle Bakken Limestone, Zone 3 - central-Middle Bakken, Zone 4 - upper-Middle Bakken Dolostone, and Zone 5 - Upper Bakken Shale. Thin sections are presented are magnified from a microscope display representing 3mm x 2mm area of shown thin sections. Last output for phase 2 is Figure 3.5 displaying a three-quarter view of the entire 3D model output from GES2016. The lowest corner of elevation represents the southwest corner target area.

Outputs for phase 3 start with the orientation of Well #16799 trajectory as imported into CMG-STARS (Figure 3.6). Figure 3.6 depicts a vertical and side view of the trajectory path as translated from GES to CMG. Figure 3.7 is the first major calibration for simulation being a curve matching analysis. Here cumulative oil production (ft³) and water cut (%) are displayed. This is a comparison of real world production history (circle and square symbols) to simulation production history (solid line and dashed line data). For an example of the CMG production history matching code look to Appendix A; all other simulation runs will be on the digital archive.

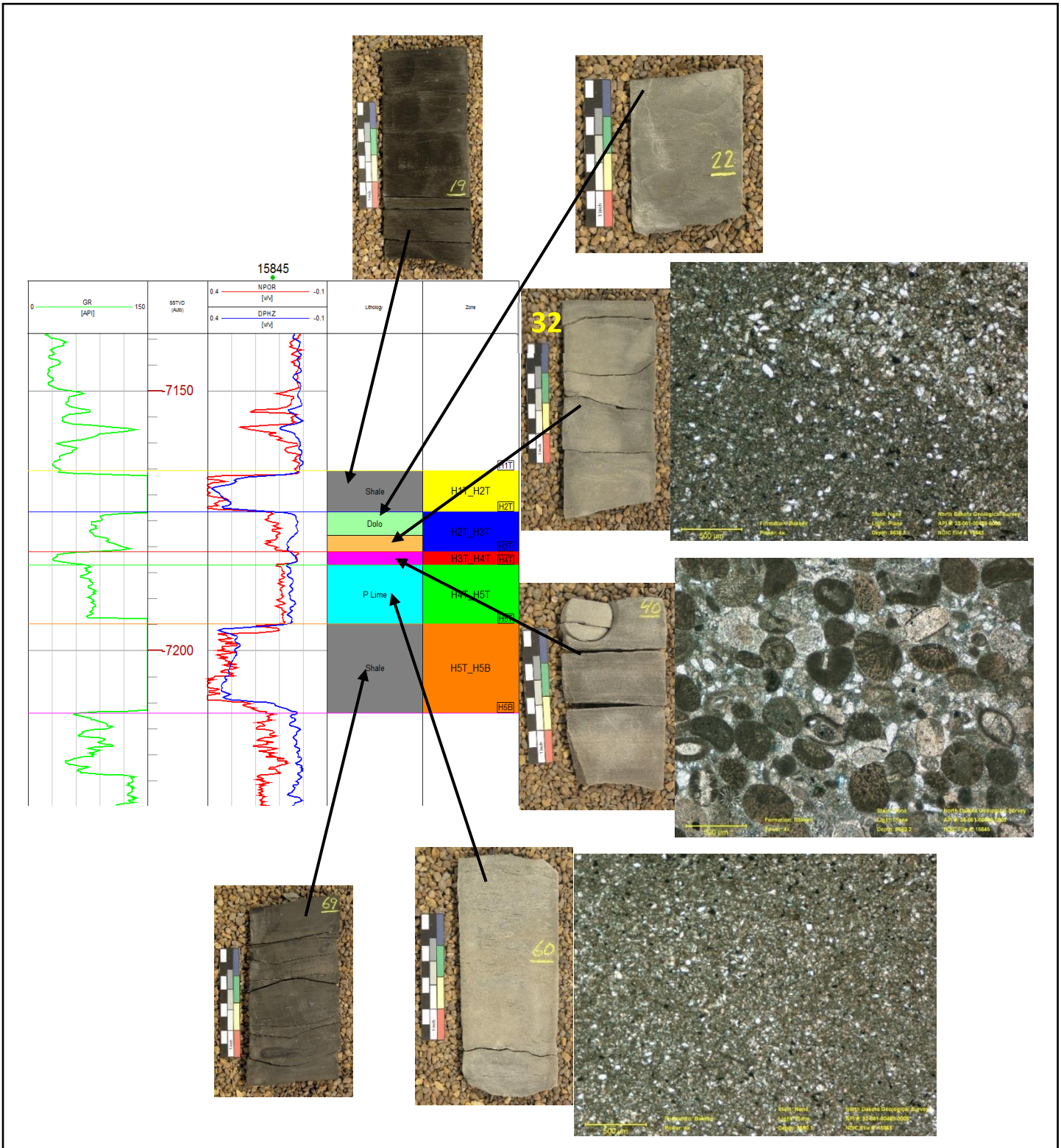


Figure 3.4: Core Comparison and Thin section observation of Bakken Rock in Core 15845. Gamma Ray, Neutron Porosity, and Density Porosity data (DMR, 2018). 5 zones of Lithofacies were generated from bottom to top are Zone 1: Lower Bakken Shale, Zone 2: lower-Middle Bakken limestone, Zone 3: central-Middle Bakken, Zone 4: upper-Middle Bakken dolostone, and Zone 5: Upper Bakken Shale. Core and thin section photos provided by UND Core library.

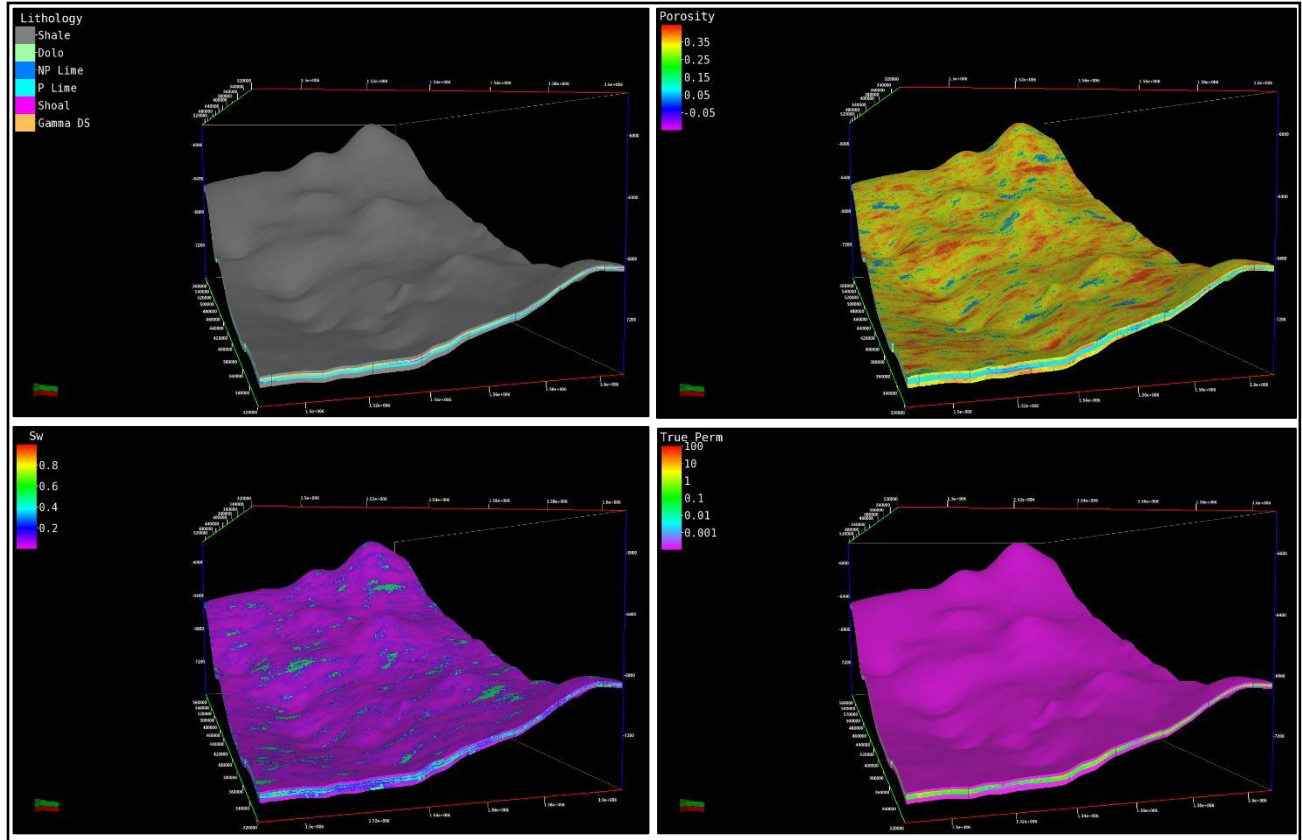


Figure 3.5: 3D view of east Mountrail County Bakken Formation. Lowest corner represents the SW corner of field area. Models show lithology, porosity, water saturation (Sw) and permeability (True Perm). All images are a 50x vertical exaggeration of elevation. Porosity correction to the Upper and Lower Bakken Shale was done CMG.

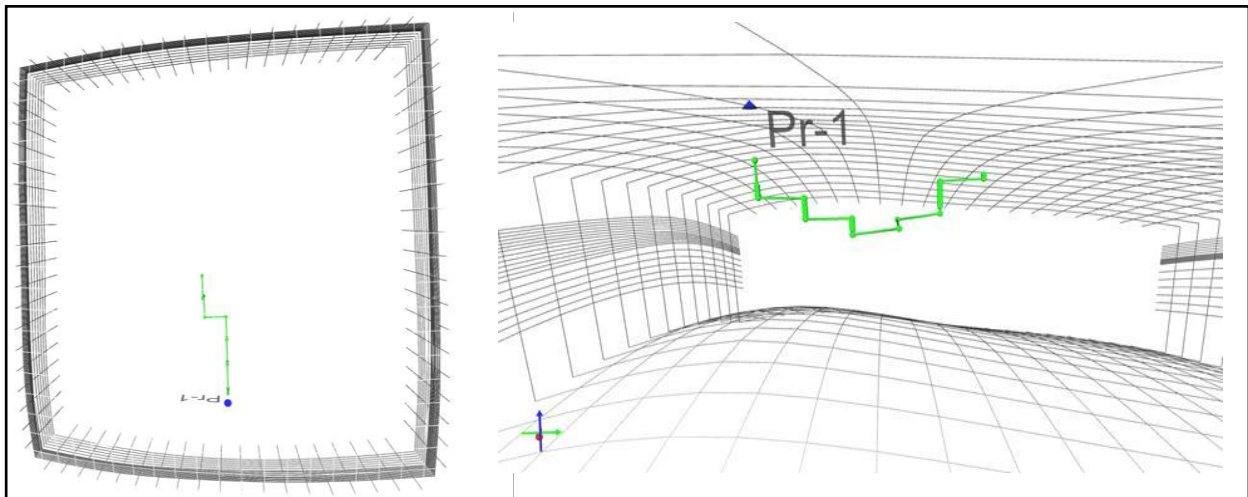


Figure 3.6: Placement and trajectory path of Well # 16799 in CMG. Map view of the numerical simulation grid is the image to the left and a side view of the numerical simulation grid is the image to the right

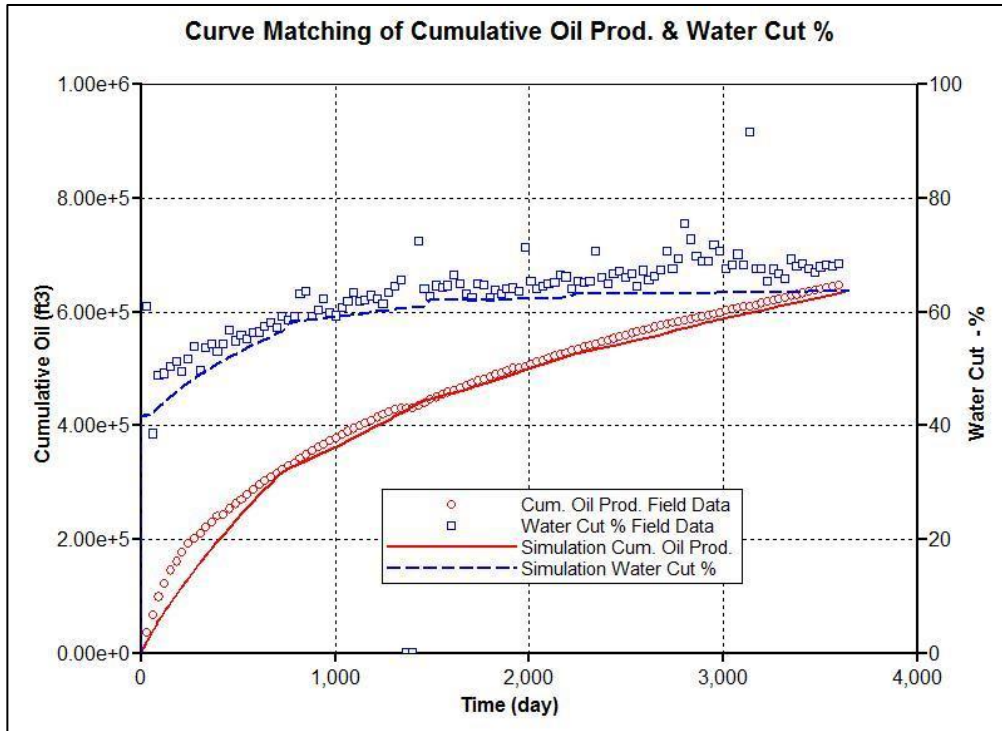


Figure 3.7: Comparison field data to simulation data for cumulative oil produced and water cut percentage. Circle symbol = real world cumulative oil production data, square symbol = real world water cut % data, red solid lines = simulated cumulative oil production data, and blue dashed line = simulated water cut % data.

The outputs from phase 4, surfactant imbibition forecasting, begin with Figure 3.8. In this graph, all the wells are running on the same injection strategy of: 30-day injection, 15-day shut-in period for solution permeation, and 90-day production. Code presented in Appendix B is added to the end of production history matching code (Appendix A) to generate a forecasting model. Figure 3.9 depicts the forecasting of different injection strategies. In Figure 3.9, the surfactant concentration is set at 1.0% for all scenarios. The scenarios are an adjustment to the injection method via injection rate, shut-in time, and production periods. For each of the forecasting scenarios, the final oil production and oil recovery factors are presented in Table 3.3. Lastly, Figure 3.10 shows the sensitivity analysis of the variables of importance, and calibration of the model from the CMG simulation. These curves show the effect of altering each variable individually by $\pm 10\%$ or $\pm 20\%$, in comparison to the fully calibrated production curve. The change in principle values show the fluctuation and effect on the overall production output.

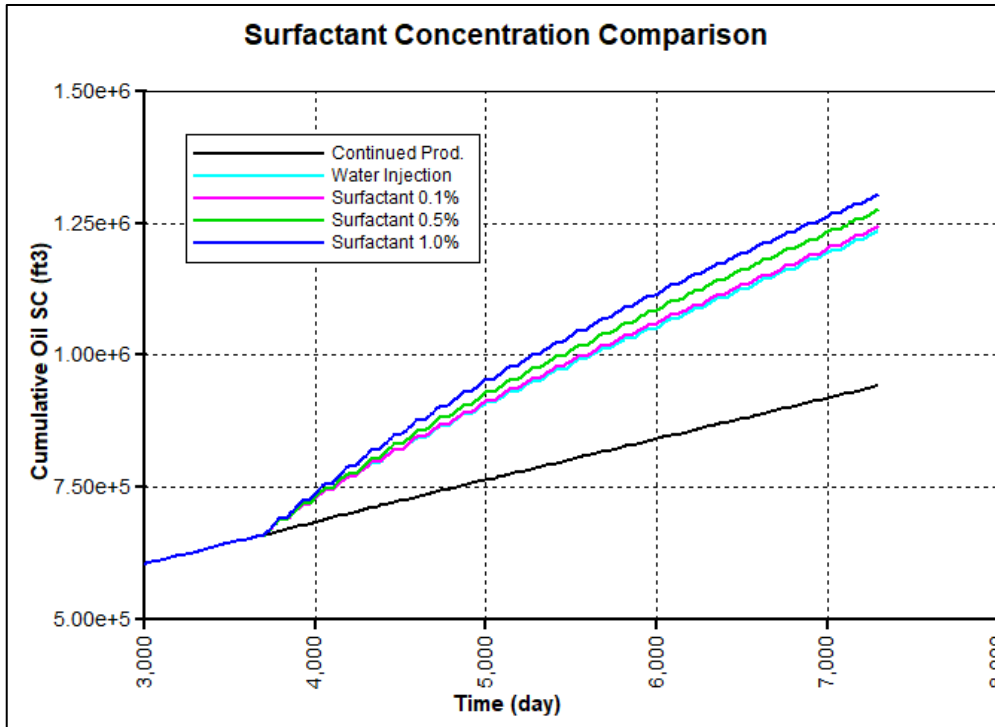


Figure 3.8: Comparison of surfactant concentrations of 0.1%, 0.5%, and 1.0% of Wang et al, 2012 nonionic surfactant formulation. The “continued production” curve is a projection of current production of the system. The “water injection” curve is modeled similar to surfactant injection, but with 0% surfactant concentration. All scenarios, except for continued production, used 30-day injection, 15-day Shut in period, and 90-day production intervals.

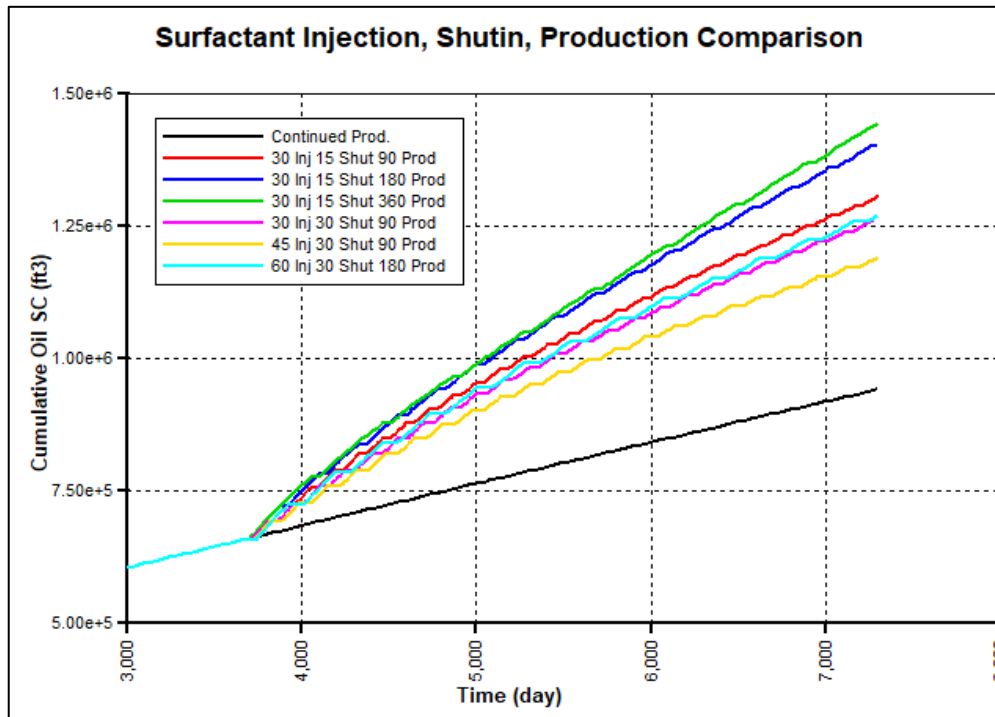


Figure 3.9: Comparison of different injection plans. Inj. = # of days of injection, Shut = # of days when well is completely shut to allow for surfactant permeation, Prod. = # of days the well is open for production. All injections of surfactant were done with 1.0% concentration.

Table 3.3: Final number of cumulative oil production and Oil Recovery factors for all forecasting scenarios. Numbers in parenthesis are Injection time, Shut in time, and Production time respectively.

Scenario	Final Cum. Oil Production (ft³)	Oil Recovery Factor %
January 1, 2018	656,783	4.4
Continued production	942,117	6.4
Water only Production (30-15-90)	1,236,600	8.4
0.1% surfactant (30-15-90)	1,245,490	8.5
0.5% surfactant (30-15-90)	1,271,220	8.7
1.0% surfactant (30-15-90)	1,306,250	8.9
1.0% surfactant (30-15-180)	1,400,430	9.5
1.0% surfactant (30-15-360)	1,444,290	9.8
1.0% surfactant (30-30-90)	1,257,800	8.6
1.0% surfactant (45-30-90)	1,191,280	8.1
1.0% surfactant (60-30-180)	1,269,530	8.6

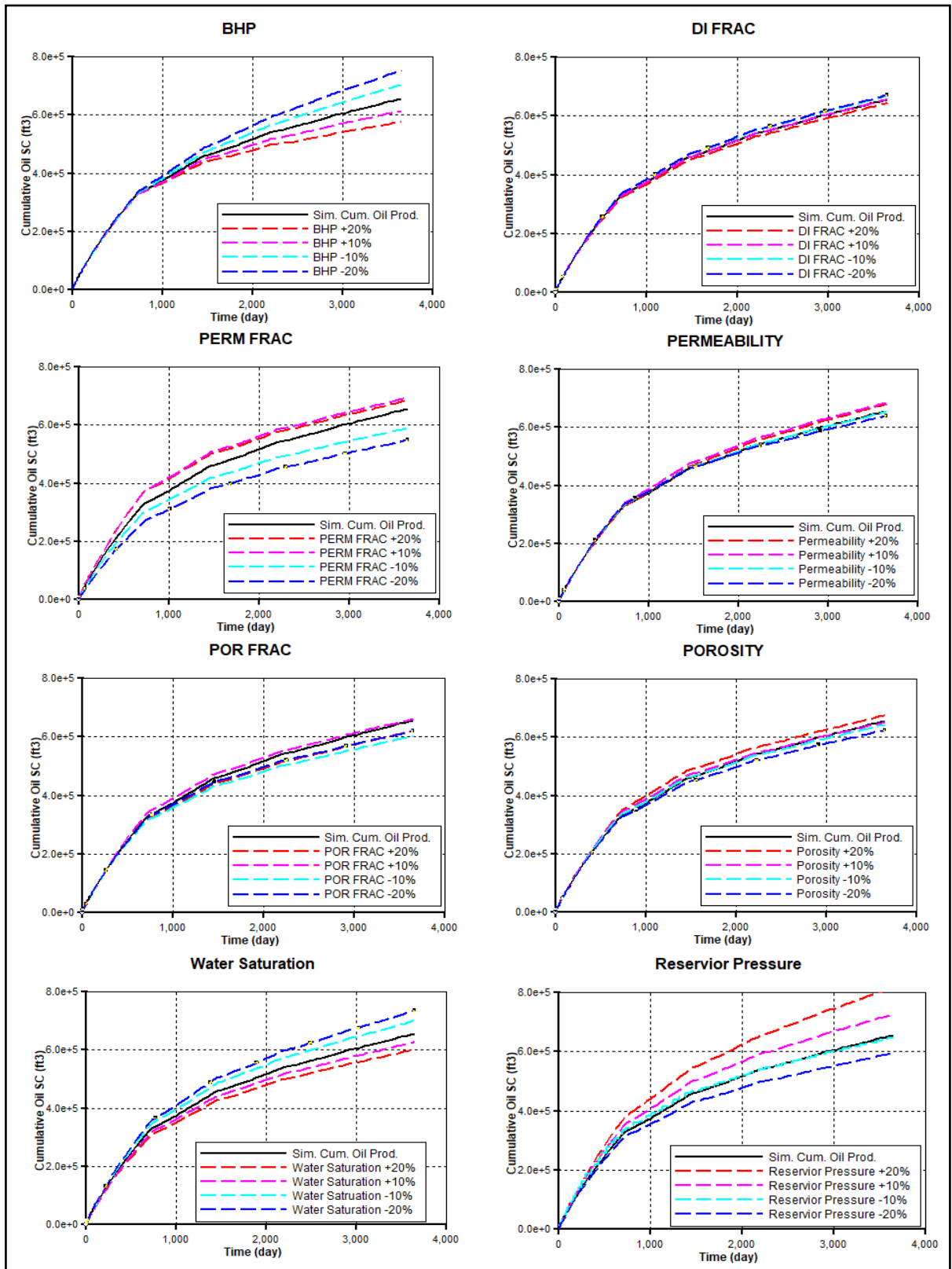


Figure 3.10: : Sensitivity analysis of bottom hole pressures (BHP), width of fractures in I-direction (DI FRAC), permeability of fractures (PERM FRAC), Permeability of all cells, porosity of fractures (POR FRAC), porosity of all cells, water saturation of system, and reservoir pressure at depth. The fractures used in the model were based on natural fractures.

CHAPTER IV

Discussion

Constructing a geological formation using a geological modeler, numerical simulator and production history match are the core focus of this research. Thus, normalizing and homogenizing heterogeneous rock during the modeling are also important steps for this research. In following the initial criteria for the hypothesis, the model generated needs to exist within real world parameters. Therefore, making sure the model follows with the depositional history and the potential lithological/petrophysical facies placement, is required for hypothesis to be successful.

For modeling Mountrail County, five zones of petrophysical facies were established. As seen in Figure 3.4, Well #15845, the five major zones of log patterns (top to bottom) were Zone 5 the Upper Bakken and Zone 4 the upper Middle Bakken siliceous dolostone. Zone 3 is the central Middle Bakken containing the clean limestone (shoal) and/or the gamma spike siliceous dolostone. Zone 2 is the lower Middle Bakken limestone, and Zone 1 is the Lower Bakken Shale. Considering past research on the deposition of these facies will help assess if the model generated is adequate. The previously stated zones do show lateral changes throughout the Bakken, specifically in zones 3 and 2 in the model. Zone 3 is the most chaotic in lateral change, where the lithologies can range from a clean limestone shoal, porous limestone, or siliceous dolostone. This can be attributed to pinch out of the shoal layers (seen in Figure 3.3) or a shift in depositional environment for Zone 2. Zone 2 showed a small lithology shift; a porous limestone and non-porous cleaner limestone. The non-porous clean limestone still had higher gamma

signature than the shoal, but similar porosity via NPOR and DPHZ signals. What all the zones amount to is a limestone base to the lower Middle Bakken, a transition to the shoal/high signature gamma dolostone in the center of the Middle Bakken, to an upper dolostone at the top of the Middle Bakken. This is likely caused by a slight sea level drop in the center of the Middle Bakken deposition, which could account for large marine fossil deposition in the shoal (Figure 3.4). Also depicted in Figure 3.4, the zone 4 dolostone layer has considerably higher porosity than the shoal (zone 3) and it is more porous than the limestone in Well #15845. This is likely from a dolomitization process. What should be noted is, in the shoal layer, there is a considerably poorly sorted grain texture dominated by fossils. This would account for the low gamma signature and low porosity. Thus, looking at the core for Well #15845, it confirms that the geophysical patterns used to correlate all 24 wells in GES2016 are effective in modeling the petrophysical facies via log pattern signatures. In modeling the Bakken, the Pronghorn member was ignored, due to the focus of the research study on the middle member of the Bakken Formation, and that the Pronghorn is not prominent in Eastern Mountrail County (Lefever, 2011). Seismic log data was considered for modeling the natural fractures. However, there were no seismic log files concentrated around Well #16799, thus it was not used for the modeling of this research but should be considered for other wells in the future if the log files are available.

Analysis of the accuracy and legitimacy of 3D modeling ultra-tight rock formations is a constant process. Starting with Figure 3.1, the southeast corner of East Mountrail County is shown to be the lowest point for the Bakken location. The illustration is in agreement with the Figure 3.5 as the interpolation from the GES2016 software matches up well with the contour of tops from ArcGIS in Figure 3.1. Figure 3.5 however, does show differences in some features when compared to the Figure 3.1, most notably in the occurrence of dome and basin structures.

Figure 3.5 represents the dome and basin structures with a 50x vertical exaggeration. This exaggeration is needed to display the downward dip structure of the Bakken in this county. In 1:1 scaling, the vertical elevation of the Bakken formation in East Mountrail County is very flat, showing little dip. The pits and hills, which illustrated in the figure, may be produced by slight mismeasurements from the Kelly Bushing readings, the measure depth of the borehole, or misplacement of the top markers of formation tops. Most likely, it's a combination of all three reasons, though care was taken to calibrate of the tops of the lithofacies and well height corrections using the drill time mud logs (DTSM) for each well. Overall based on the GES2016 3D model output and the correlation to real world core comparison the Geological model is successful in existing within real world parameters.

After having built a reasonable 3D model of the Bakken, next was to make sure it matched previous production history, to calibrate its forecasting potential (Figure 3.7). Figure 3.7 overall is a good fit between the natural production data provided by Hunt Oil Company and the simulation model data that was established. However, Figure 3.7 also displays a slight deviation, which is likely due to the irregular shut downs of Well # 16799. This point is clearly seen around day 1400 in the cumulative history with water cut at 0% and no cumulative oil increase. However, in the simulation, within the time frame the well was put in use from March 1st, 2008 to December 31st, 2017 before EOR effectiveness prediction, the relative errors of cumulative oil production is 0.296%, and the water cut is 4.164%, respectively. The relative errors are less than 7%. Thus, based on the initial criteria the model is a success according to the numerical simulation experience and standard for history match. Overall, the trending of cumulative oil production and water cut matches well with production history.

Now that the model's initial production is calibrated to the known history, forecasting becomes possible. Figure 3.8 presents the effects of surfactant concentration on the production of Well #16799. As it shows, 1.0% surfactant concentration produces the most oil in the 10-year period over the other concentrations with ORF of 8.9%. However, even though it has the greatest recovery potential, the amount of surfactant it needs would be roughly 15,000 ft³ of pure nonionic surfactant over a ten-year period to reach this result. Thus, the potential to use any of these surfactant solutions becomes a question of cost efficiency, with the price of surfactant solution at the given time of inquiry and the cost of labor for injection versus the potential gains in oil production. In general, the surfactants improve the overall recovery of oil in the well compared to the continued projected trend, and also surpasses water only injection method. Though it should be noted that the water injection simulation method does not account for clay swelling found in Wang et al, 2011 and 2012, thus the water only injection projection output is overestimated.

In addition to surfactant concentrations, injection strategies play a large part in the effectiveness of Surfactant EOR. Figure 3.9 shows the effects of changes in injection time, Shut-in time and Production time intervals. As it shows 30-day injection, 15-day shut-in, and 360-day production shows the best overall recovery totals over the other methods. One large component as to why this combination has the best result is due to the larger production time period after a shorter injection/shut-in time as compared to the other methods. This means that there is less time spent with no production (injection/ shut in time) and more time with the well open to extract oil. However, the injection is still affecting the system when compared to the continuous production results. Without surfactant stimulation, the forecasted production is much lower. In addition, the production period in the "30-15-360" huff-n-puff strategy may need to be adjusted

in case of mechanical problems according to the real-world application. In Table 3.3 it clearly shows that the oil recovery factor jumps from a predicted 4.4% ORF to 9.8% ORF with the optimized EOR method, producing roughly 800,000 ft³ more of oil. Note that the injection times of 45 and 60 days had cumulative oil production is greater than the continued production model, but is lower overall cumulative oil production. Thus, as long as injection time, and shut-in time are maximized for efficiency to the time of production, large improvements in oil recovery hypothetically could be obtained in Well #16799. On the other hand, during the practical well operation, the engineers also need to consider the pump capability and mechanical issues for the frequency of well to open or closed.

The next step was the sensitivity analysis. Figure 3.10 displays the responses to variable changes of the initial curve matching by a $\pm 10\%$ or $\pm 20\%$ change in individual variables to the simulation. As Figure 3.10 depicts, all of the variables influence the curves output, and they need to be considered for an accurate model. Specifically, bottom hole pressure, fracture permeability, water saturation, and reservoir pressure play the largest roles in calibrating this simulation. Thus, the accuracy of these variables need to be evaluated. As depicted in Table 3.2, the BHP calculated with equation (4) from the production data falls within the used BHP values in the simulation. It should be noted that the simulation does go higher in BHP than what the production history shows, but since the difference in values are less than 10% and that the model is homogenizing a large areas causing possible errors, this difference is negligible. Water saturation data was generated directly from log calculations using equations (1) and (2), thus solidifying it as accurate. As for reservoir pressure and fracture permeability, no direct correlations from Well #16799 were used to reference these values. However, reservoir pressure was indirectly determined via the relationship of pressure vs depth, along with the notion that the

Bakken is overpressured from capillary forces, as theorized by Nordeng et al. 2010, to be about 6300 psi. This is only a 5% increase from our model. As for the fracture permeability, this was a trial and error type of curve matching technique and could be refined better with more data about the nature of fractures caused by hydraulic fracturing of ultra-tight rock, provided by well companies. With this model having fracture permeability of 0.01md, it is well within the range of possibilities of being generated. In regard to the variables that do not have a large sensitive impact on the model, they should not be ignored either. Porosity, for example, is intrinsic to the amount of oil in-place, along with being a variable to water saturation and permeability. Thus, all variables in Figure 3.10 need to be considered for model generation and simulation. It should be noted that CMG-CMOST would do a similar job to analyzing the sensitivity of the simulation models, but due to time constraints it could not be implemented for this research. Future work on this topic would benefit greatly by using CMG-CMOST in criticizing their model's viability.

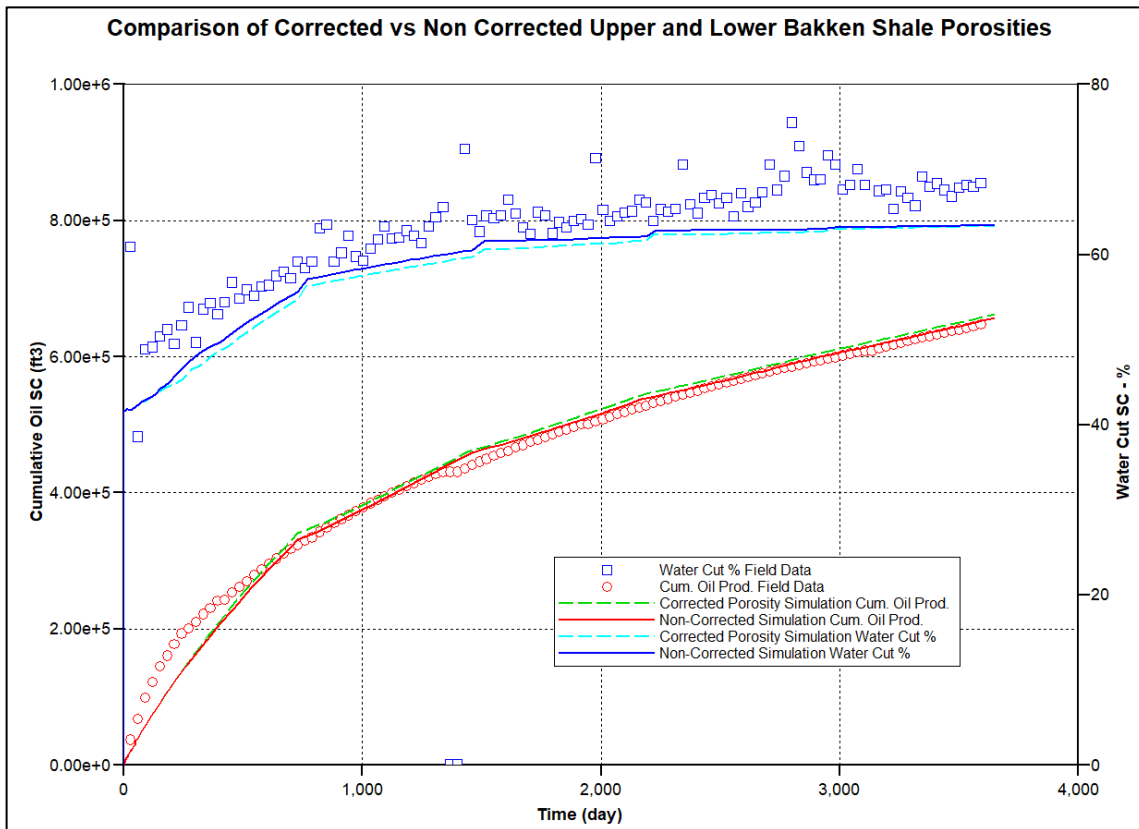


Figure 4.1: Comparison of corrected shale porosity vs. non-corrected shale porosity. Red and green curves are simulation results of oil accumulation and red circles represent field data cumulative results. Dark and light blue curves are simulation results of water cut percentage and blue squares are field data water cut percentage.

Along with the sensitivity analysis refer back to Table 2.2. The shale porosity values were corrected post GES2016 modeling in CMG. As you can see in Figure 3.5, the model has large values for the porosity of the Upper and lower shales. These calibrations should be done in GES2016 before exporting to CMG. Comparisons of non-corrected porosity and Corrected porosity can be seen in Figure 4.1. Although Figure 4.1 shows no change significant change in production history with changes in shale porosity for the Upper and lower Bakken Shales, this does not mean corrections should be done in CMG. The Porosity Corrections should be dealt with in Phase 2 with geological modeling. In future work on this topic the error generated from equation 1 for shales units in the Bakken should be calibrated to core analysis prior to numerical modeling.

The last step for the model is to evaluate if the production increase shown in the simulation of Well #16799 is considered profitable. Using the US Department of Energy Cost break down of Injection systems, (Godec, 2014), the costs of implementing the surfactant system is seen in Table 4.1. In Godec, 2014 average assumption of Installation costs (Installation, Fluid management, and operations & maintenance), Lifting energy costs (energy to extract all fluids from the system), and Injection energy costs were made based on US department of energy averages. Surfactant price was based on the 2017 industry standard for nonionic surfactants and oil prices were based on June 25th, 2018 price of oil per bbl. Table 4.1 shows that all injection strategies show positive net profit. However, these are only rough calculations based on national averages; thus, if increases in surfactant costs, energy costs or complications in maintaining these systems, could increase the overall net profit will decrease. That being said, most of the strategies implemented show a return on investment of 1.48 to 3.77, meaning that with the proper injection strategy there could potentially be a 3.77 times return in investment. Overall, the crude

cost analysis shows that there is a possible profit gain to be had from the surfactant imbibition simulation.

Table 4.1: Cost and profit comparison of implementing surfactant EOR strategies. Costs were generated from averages of installing and running fluid injection systems from US Department of Energy (Godec, 2014). Gross profit is the profit accumulated above the continuous production forecast.

Strategy	Costs estimates for 10 years	Gross profit compared to Continuous model for 10 years	Net profit after 10 years	Profit/ Cost Ratio
0.1% conc. 30-15-90	\$1.36 Million	\$3.58 Million	+ \$2.22 Million	2.63
0.5% conc. 30-15-90	\$1.50 Million	\$4.01 Million	+ \$2.51 Million	2.67
1% conc. 30-15-90	\$2.02 Million	\$4.43 Million	+ \$2.41 Million	2.20
1% conc. 30-15-180	\$1.82 Million	\$5.58 Million	+ \$3.76 Million	3.07
1% conc. 30-15-360	\$1.62 Million	\$6.11 Million	+ \$4.49 Million	3.77
1% conc. 30-30-90	\$1.95 Million	\$3.84 Million	+ \$1.89 Million	1.97
1% conc. 45-30-90	\$2.05 Million	\$3.03 Million	+ \$0.98 Million	1.48

Conclusions

The basis of this research was two-fold: 1) To see if an ultra-tight rock formation, such as the Bakken Fm., could be modeled and simulated with production history matching real world production. 2) To see if surfactant imbibition could be a viable future option for a well in the Bakken Formation (i.e. Patten 1-27H, Well # 16799). Based on the preliminary result, several conclusions can be made as follows:

- (1) Based on the initial criteria for the hypothesis, we could successfully scale to Wang et al., 2012's lab results in terms of ORF values of 6 to 20% oil recovery factor in simulation.
- (2) Modeling of an ultra-tight formation and matching production history is possible.
- (3) Based on the research results, the simulation shows that surfactant imbibition might be able to improve production of oil both cumulative oil and ORF for ultra-tight rocks for the Well #16799 by about 9.8% ORF. The simulation result shows a favorable potential using surfactant EOR method to increase oil recovery for the Bakken Formation.
- (4) Integrated software with geological and reservoir properties (e.g. GES2016 and CMG-STARS) is a plausible method of modeling and simulating ultra-tight rock formations,

and can be used to simulate further EOR techniques such as surfactant imbibition for other wells.

(5) Based on rough cost to profit analysis, Well #16799 could see a potential profit increase if the surfactant imbibition system was implemented.

(6) Future work must be done to support or edit this model and research. The next stage would be to implement a surfactant injection system in a real world, for a currently producing well to see if the results match with the findings of this research.

Nomenclature

ϕ_e = Effective porosity (%)

ϕ_D = Density porosity

ϕ_N = Neutron porosity

S_w = Water Saturation (%)

a = Tortuosity component [Unit less]

n = Saturation exponent (varies from 1.8 to 4.0) [unit less]

m = Cementation exponent (varies from 1.7 to 3.0) [unit less]

R_w = Resistivity of formation water at formation temperature

R_t = True resistivity of the formation

K = Permeability [md]

C = Permeability constant

D = Porosity constant

E = irreducible saturation exponent

BHP = Bottom hole pressure (psi)

TDS = Total Dissolved Salinity

TVD = True vertical depth (ft)

OOIP = Original oil in place

ORF = Oil recovery factor

REFERENCES

1. Asquith, G.B., and Gibson, C., 1982. Basic Well Log Analysis for Geologists. *American Association of Petroleum Geologists*. Tulsa, Oklahoma.
2. Blakey, Ron, 2011. Paleogeography of North America from 560 Million Years Ago to Today. PPT.
3. Blakey, Ron, 2013. Using Paleogeographic Maps to Portray Phanerozoic Geologic and Paleotectonic History of Western North America. *AAPG article #30267, Presented March 26, 2013*. PPT
4. Crain, E.R., 2015. Crain's Petrophysical Handbook. <https://www.spec2000.net/> November, 2017.
5. DMR, 2018. Department of Mineral Resources Oil and Gas Division <https://www.dmr.nd.gov/oilgas/feeservices/getscoutticket.asp> April 7, 2018.
6. Doveton, J., 1999, Basics of Oil and Gas Log Analysis. *Kansas Geological Survey*. http://www.kgs.ku.edu/PRS/Info/pdf/oilgas_log.html, November 2017.
7. Gaswirth, S., Marra, K., Cook, T., Charpentier R., Gautier, D., Higley, D., Klett, T., Lewan, M., Lillis, P., Schenk, C., Tennyson, M., and Whidden, K. 2013 Assessment of Undiscovered Oil Resources in the Bakken and Three Forks Formations, Williston Basin Province, Montana, North Dakota, and South Dakota, 2013. *US Geological Survey National Assessment of Oil and Gas Fact Sheet*.
8. Godec, M., 2014. Acquisition and Development of Selected Cost Data for Saline Storage and Enhanced Oil Recovery (EOR) Operations. *US Department of Energy: National Energy Technology Laboratory (NETL) DOE/NETL-2014/1658. p. 1-19*
9. Harwell, J.H., Sabatini, D.A., and Knox, R.C., 1999, Surfactants for Ground Water Remediation. *Colloids and Surfaces, A: Physicochemical and Engineering Aspects*, Vol 151, p. 255-268.
10. Jin, H., and Sonnenberg, S.A., 2015. Characterization for Source-Rock Potential of the Bakken Shales in the Williston Basin. *Unconventional Resources Technology Conference 2015 URTeC: 2169797*.

11. Lefever, J., Lefever, R., and Nordeng, S., 2013. Chapter 1 Revised Nomenclature for the Bakken Formation (Mississippian-Devonian), North Dakota. *The Rocky Mountain Association of Geologists*. p. 11-26
12. Lefever, J., 2008. What's Happening at Parshall, North Dakota. *Department of Mineral Resources Newsletter*, Vol. 35 No. 1 P. 1-2.
13. Malmsten, M., 2002, Surfactants and Polymers in Drug Delivery. *Taylor & Francis Group, LLC*. Boca Raton, FL. Pg. 1-3.
14. Nordeng, S., 2010. A Brief History of Oil Production from the Bakken Formation in Williston Basin. *North Dakota Department of Mineral Resources Geo News*. Volume 37 No. 1 p. 5-9.
15. Nordeng, S., Lefever, J.A., Anderson, F.J., and Johnson, E.H., 2010. An Examination of the Factors that Impact Oil Production from the Middle Member of the Bakken Formation in Mountrail County, North Dakota. *North Dakota Geological Survey*. No. 109 p. 1-89.
16. Pitman, J.K., Price, L.C., LeFever, J.A., 2001. Diagenesis and Fracture Development in the Bakken Formation, Williston Basin: Implications for Reservoir Quality in the Middle Member. *U.S. Geological Survey*. p. 1-19.
17. Pollastro, R.M., Roberts, L.N.R., and Cook, T.A., 2013. Chapter 5 Geologic Assessment of Technically Recoverable Oil in the Devonian and Mississippian Bakken Formation. *U.S. Geological Survey*. p. 1-34.
18. Rai, S.K., Bera, A., and Mandal, A., 2015. Modeling of Surfactant and Surfactant-polymer Flooding for Enhanced Oil Recovery using STARS (CMG) software. *Springer, J Petrol Explor Technol* 1:5-11.
19. Ramakrishna, S., Balliet, R., Miller, D., Halliburton, S.S., and Merkel, D., 2010 Formation Evaluation in the Bakken Complex Using Laboratory Core Data and Advanced Logging Technologies. *SPWLA 51st Annual Logging Symposium SPWLA-2010-74900*. p. 1-16
20. Romadhona, M., Octaviany, K.T., and Jaya, P., 2013. A Study to Formulate Predictive Model and Screening Criteria for New EOR Method in Indonesia: Surfactant Huff N' Puff Injection. *IPA 37th Annual Convention IPA13-SE-017*.
21. Rosen, M.J., Kunjappu, J.T., 2012. Surfactants and Interfacial Phenomena 4th Edition. *John Wiley & Sons, Inc*. Hoboken, New Jersey

22. Schlumberger, 2009. Log Interpretation Charts 2009 Edition: Gen-6 Resistivity of NaCl Water solutions. *Schlumberger, Sugar land, Tx.* p. 8
23. Selley, R.C., and Sonnenberg, S.A, 2014. Elements of Petroleum Geology Third Edition. *Elsevier Inc.*
24. Simenson, A., Sonnenberg, S.A., Cluff, R.M., 2013. Bakken Guidebook Chapter 3: Depositional Facies and Petrophysical Analysis of the Bakken Formation, Parshall Field and Surrounding Area, Mountrail County, North Dakota. *The Rocky Mountain Association of Geologists.* p. 48-101.
25. Smith, M.G. and Bustin, R.M. 2000. Late Devonian and Early Mississippian Bakken and Exshaw Black Shale Source Rocks, Western Canada Sedimentary Basin: A Sequence Stratigraphic Interpretation. *AAPG Bulletin.* vol. 84, no. 7, p. 940-960.
26. Sonnenberg, S.A. 2017. Sequence stratigraphy of the Bakken and Three Forks Formations Williston Basin, USA. *AAPG Rocky Mountain Section Meeting Article #10990 PPT.*
27. Sonnenberg, S.A and Pramudito, A., 2009. Petroleum Geology of the giant elm Coulee Field, Williston Basin. *AAPG Bulletin,* vol. 93, no. 9, p. 1127-1153.
28. Yu, W., Lashgari, H.R., Sepehrnoori, K., 2014. Simulation Study of CO₂ Huff-n-Puff in Bakken Tight Oil Reservoirs. Paper SPE-169575-MS was presented at the SPE Western North American and Rocky Mountain Joint Regional Meeting held in Denver, Colorado, USA. 16-18 April.
29. Wang, D., Butler, R., Liu, H., and Ahmed, S., 2011. Surfactant Formulation study for Bakken Shale Imbibition. Paper SPE-145510-MS was presented at the SPE Annual Technical Conference and Exhibition, Denver, Colorado, USA. 30 October-2 November.
30. Wang, D., Butler, R., Zhang, J., Seright, R., 2012. Wettability Survey in Bakken Shale with Surfactant-Formation Imbibition. *SPE Reservoir Evaluation & Engineering,* Volume 15(6), p. 695-705.
31. Wang, D., Zhang, J., Butler, R., Olatunji, K., 2016, Scaling Laboratory Data Surfactant-Imbibition Rates to the Field in Fractured-Shale Formations. *SPE Engineering & Evaluation,* August, Volume 19 (03), p.441-449.

APPENDIX A

Production History Matching Simulation Code:

```
** ===== INPUT/OUTPUT CONTROL =====

RESULTS SIMULATOR STARS

*INTERRUPT *STOP

*TITLE1 'Surfactant Model for Bakken East Mountrial County'

*INUNIT *FIELD *EXCEPT 2 1 ** deg C instead of deg F
          *EXCEPT 7 0 ** kg instead of lb
          *EXCEPT 8 0 ** gmo1 instead of lbmo1
          *EXCEPT 11 1 ** ft3 instead of bbl

** Additional information on mechanisms obtained from special printouts
*OUTPRN *GRID *PRES *SW *SO *SG *TEMP *X *W *OBHLOSS *ADSORP
          *MASDENO *MASDENG *MASDENW *KRINTER *IFT
          *MASFR *ADSPCMP ** special adsorption composition, in mass
fraction
*OUTPRN *WELL *ALL
*WRST 100
*WPRN *GRID 100
*WPRN *ITER 100
*WPRN *SECTOR 100
*WSRF *SECTOR TIME

*OUTSRF *WELL *COMPONENT *ALL
*OUTSRF *GRID *PRES *SW *SO *SG *TEMP
          *MASDENO *MASDENG *MASDENW *KRINTER *IFT
          *MASFR *ADSPCMP ** special adsorption composition, in mass
fraction

** ===== GRID AND RESERVOIR DEFINITION =====

GRID CORNER 20 20 20
CORNERS
INCLUDE 'CORNER.txt'

***** Input by w*****

*DIFRAC *CON 0.01          ** Reservoir has vertical fractures only
*DJFRAC *CON 122
*DKFRAC *CON 3.05

*DUALPERM

PERMI MATRIX ALL
INCLUDE 'PERM.txt'
```

```
*PERMJ *MATRIX *EQUALSI
*PERMK *MATRIX *EQUALSI * 0.01
```

```
*PERMI *FRACTURE *IJK
1:20 1:20 1:20 0.0000001
```

```
*MOD
11:11 5:5 1:5 = 0.01
11:11 6:6 5:10 = 0.01
11:11 7:7 10:14 = 0.01
11:11 8:8 14:14 = 0.01
10:10 8:8 14:14 = 0.01
10:10 9:9 3:14 = 0.01
10:10 10:10 2:3 = 0.01
```

```
*PERMJ *FRACTURE *IJK
1:20 1:20 1:20 0.0000001
```

```
*MOD
11:11 5:5 1:5 = 0.01
11:11 6:6 5:10 = 0.01
11:11 7:7 10:14 = 0.01
11:11 8:8 14:14 = 0.01
10:10 8:8 14:14 = 0.01
10:10 9:9 3:14 = 0.01
10:10 10:10 2:3 = 0.01
```

```
*PERMK *FRACTURE *IJK
1:20 1:20 1:20 0.0000001
```

```
*MOD
11:11 5:5 1:5 = 0.01
11:11 6:6 5:10 = 0.01
11:11 7:7 10:14 = 0.01
11:11 8:8 14:14 = 0.01
10:10 8:8 14:14 = 0.01
10:10 9:9 3:14 = 0.01
10:10 10:10 2:3 = 0.01
```

```
** 0 = null block, 1 = active block
NULL CON 1
```

```
POR MATRIX ALL
INCLUDE 'POR.txt'
```

```
*POR *FRACTURE *IJK
1:20 1:20 1:20 0.00001
```

```
MOD
11:11 5:5 1:5 = 0.1
11:11 6:6 5:10 = 0.1
11:11 7:7 10:14 = 0.1
11:11 8:8 14:14 = 0.1
10:10 8:8 14:14 = 0.1
10:10 9:9 3:14 = 0.1
10:10 10:10 2:3 = 0.1
```

```
*****
SECTOR 'AREA'
10:11 5:10 1:14
*****
```

```
** 0 = pinched block, 1 = active block
```

PINCHOUTARRAY CON

1

*END-GRID

*PRPOR 3600

*ROCKCP 63

*THCONR 43.2

*THCONW 43.2

*THCONO 43.2

*THCONG 43.2

** Because of cold water injection, heat flows in from over/underburden

*HLOSSPROP *OVERBUR 63 43.2 *UNDERBUR 63 43.2

** ===== FLUID DEFINITIONS =====

*MODEL 4 4 4 ** North Sea light oil

*COMPNAME	'WATER'	'CHEM'	'OIL'	'GAS'
**	-----	-----	-----	-----
*CMM	0.018	0.706	0.585	0.028
*MOLDEN	1566	65.56	158.84	730
*CP	3e-6	3e-6	1e-6	1e-6
*CT1	2.33e-4	2.33e-4	1e-4	1e-4
*PCRIT	3200	632	453	492.4
*TCRIT	374	134	175	-147
*CPL1	0	0.2417	0.2417	0.008815

*RANGECHECK *OFF

*SOLID_DEN 'CHEM' 28190.8 0 0

*RANGECHECK *ON

*SOLID_CP 'CHEM' 0.016112889 0 ** (17 J/gmole-C) * (1 Btu / 1055.056 J)

**LIQPHASE

**PRSR 25.40

**TEMR 82.02

**PSURF 14.65

**TSURF 20

*WATPHASE

*VISCTABLE

**Temp TDS:298,750 ppm

15	0	2.46	1.87	2.44
20	0	2.16	1.726	2.24
30	0	1.71	1.704	2.04
40	0	1.38	1.229	1.98
50	0	1.14	1.022	1.76
60	0	0.95	0.933	1.53
70	0	0.80	0.768	1.23
80	0	0.69	0.665	1.13
90	0	0.60	0.571	0.94
100	0	0.53	0.477	0.76
110	0	0.47	0.393	0.76

120	0	0.42	0.343	0.76
130	0	0.38	0.319	0.76
330	0	0.18	0.119	0.46

*Xnacl 0.10
 *OILPHASE
 *VISCTABLE
 **Temp

15	2.46	2.46	1.87	2.44
20	2.16	2.16	1.726	2.24
30	1.71	1.71	1.704	2.04
40	1.38	1.38	1.229	1.98
50	1.14	1.14	1.022	1.76
60	0.95	0.95	0.933	1.53
70	0.80	0.80	0.768	1.23
80	0.69	0.69	0.665	1.13
90	0.60	0.60	0.571	0.94
100	0.53	0.53	0.477	0.76
110	0.47	0.47	0.393	0.76
120	0.42	0.42	0.343	0.76
130	0.38	0.38	0.319	0.76
330	0.018	0.18	0.119	0.46

*LIQPHASE
 *PRSR 7000
 *TEMR 95
 *PSURF 14.7
 *TSURF 23
 *GASLIQKV ** The following are gas-liquid K values

***KVTABLIM 580 4640 5 100
 **KVTABLIM 580 6980 5 100
 KVTABLIM 580 6400 5 100

*KVTABLE 'WATER' ** want no water in gas phase (override default)
 8*0
 8*0

*KVTABLE 'GAS'
 1.733 1.27 1.049 0.918 0.785 0.757 0.705 0.685
 3.895 2.944 2.437 2.132 1.825 1.759 1.639 1.592

*LIQLIQKV ** The following are the liquid-liquid K values at 5 concentrations

*KVTABLIM 3000 9000 5 100
 kvkeycomp 'CHEM' global 0 0.008

*KVTABLE 'WATER' ** Each component has a P-T dependent table at
 *KEYCOMP ** the following values of z(CHEM):
 2*0.
 2*0. ** 0.0 0.002 0.004 0.006 0.008
 *KEYCOMP
 2*7E-4
 2*7E-4
 *KEYCOMP
 2*0.0037
 2*0.0037

```

*KEYCOMP
  2*0.0125
  2*0.0125

*KEYCOMP
  2*0.0398
  2*0.0398

*KVTABLE 'CHEM'
  *KEYCOMP
    2*0.1
    2*0.1
  *KEYCOMP
    2*0.1458
    2*0.1458
  *KEYCOMP
    2*0.1741
    2*0.1741
  *KEYCOMP
    2*0.2204
    2*0.2204
  *KEYCOMP
    2*0.3025
    2*0.3025

*KVTABLE 'OIL'
  *KEYCOMP
    2*1E-4
    2*1E-4
  *KEYCOMP
    2*0.0314
    2*0.0314
  *KEYCOMP
    2*0.1214
    2*0.1214
  *KEYCOMP
    2*0.259
    2*0.259
  *KEYCOMP
    2*0.433
    2*0.433

*KVTABLE 'GAS'
  *KEYCOMP
    2*1E-4
    2*1E-4
  *KEYCOMP
    2*0.0314
    2*0.0314
  *KEYCOMP
    2*0.1214
    2*0.1214
  *KEYCOMP
    2*0.259
    2*0.259
  *KEYCOMP
    2*0.433
    2*0.433

** Since component CHEM's w/o K value is less than 1, the default *SURFLASH

```

** assumes all CHEM's SR2 reporting is in the oil phase. Force CHEM's
 ** surface phase to be water to match the injection.
 SURFLASH W W O G

*ROCKFLUID

** ===== ROCK-FLUID PROPERTIES =====

*RPT 1 ** ----- MATRIX -----

** Interpolation between 2 sets: high versus low IFT situations.

*INTCOMP 'CHEM' *OIL

*INTLIN ** Linear interpolation of X(surfactant)

*IFTTABLE ** Surfactant chosen to work best at initial reservoir T

*TEMP 5 ** 5 deg C Table

**	oil mole frac	IFT
**	-----	-----
	0.	30
	0.0005	3
	0.001	0.3
	0.002	0.03
	0.003	0.003
	0.004	0.003

*TEMP 95 ** 95 deg C Table

**	oil mole frac	IFT
**	-----	-----
	0.	10
	0.0005	1
	0.001	0.1
	0.002	0.01
	0.003	0.001
	0.004	0.001

** Set #1: High IFT, corresponding to no surfactant

** -----

*KRINTRP 1

OILWET

**DTRAPW -4

**DTRAPN -4.222 ** Critical cap num for detrapping to begin

DTRAPW -7.22185

DTRAPN -7.22185

*SWT ** water-oil relative permeabilities

**	Sw	Krw	Krow
**	-----	-----	-----
	0.22	0.	0.842
	0.3	0.420	0.721
	0.4	0.530	0.479
	0.5	0.580	0.254

0.6	0.625	0.15
0.65	0.65	0.

*SLT ** Liquid-gas relative permeabilities

** S1	Krg	Krog
0.4	0.35	0.
0.5	0.287	0.179
0.6	0.225	0.357
0.65	0	0.65

** Set #2: Low IFT, corresponding to high surfactant concentration

**-----
*KRINTRP 2

WATWET

DTRAPW -0.63827

DTRAPN -2.92082

**DTRAPW -1.68

**DTRAPN -2.222 ** Critical cap num for complete detrapping

*SWT ** water-oil relative permeabilities

** Sw	Krw	Krow
0.0	0.0	1.
0.1	0.1	0.9
0.2	0.2	0.8
0.3	0.3	0.7
0.4	0.4	0.6
0.5	0.5	0.5
0.6	0.6	0.4
0.7	0.7	0.3
0.8	0.8	0.2
0.9	0.9	0.1
1.	1.0	0.

*SLT ** Liquid-gas relative permeabilities

** S1	Krg	Krog
0.0	1.	0.
0.1	0.9	0.1
0.2	0.8	0.2
0.3	0.7	0.3
0.4	0.6	0.4
0.5	0.5	0.5
0.6	0.4	0.6
0.7	0.3	0.7
0.8	0.2	0.8
0.9	0.1	0.9
1.	0.	1.

** Adsorption Data

**-----

```

*ADSCOMP 'CHEM' *WATER ** Reversible adsorption of aqueous surfactant
*ADSLANG *TEMP ** Langmuir isotherms at 2 temperatures
  5 20 0 1000
  95 2 0 1000
*ADMAXT .02 ** No flow modifications from adsorption

*RPT 2 ** ----- FRACTURE -----

*SWT ** water-oil relative permeabilities

** Sw      Krw      Krow
** ----    - - - - -
  0.0      0.0      1.0
  1.0      1.0      0.0

*SLT ** Liquid-gas relative permeabilities

** sl      Krg      Krog
** ----    - - - - -
  0.0      1.0      0.0
  1.0      0.0      1.0

** Assign rel perm sets

*KRTYPE *MATRIX *CON 1
*KRTYPE *FRACTURE *CON 2

*INITIAL

** ===== INITIAL CONDITIONS =====

** Automatic static vertical equilibrium
vertical depth_ave
*REFPRES 6000.0
*REFBLOCK 10 10 5

** oil reservoir has gas cap above and aquifer below
INITREGION 1
SW ALL
INCLUDE 'SW.txt'
*MOD * 0.98

*TEMP *CON 93.3
*MFRAC_GAS 'GAS' *CON 1
*MFRAC_OIL 'OIL' *CON 0.4
*MFRAC_OIL 'GAS' *CON 0.6

*NUMERICAL

** ===== NUMERICAL CONTROL =====

** All these can be defaulted. The definitions
** here match the previous data.

*SDEGREE 1
*TFORM *ZT
*DTMAX 61

*NORM      *PRESS 150 *ZO .1 *TEMP 50 *ZNCG .1 *ZQA .1

```

*RUN

** ===== RECURRENT DATA =====

*TIME 0

*DTWELL 1

*WELL 1 'Pr-1'

*WELL 2 'In-1'

*PRODUCER 'Pr-1'

*OPERATE *STO 2192

**OPERATE *STL 4384

*OPERATE MIN BHP 0.01 CONT

** rad geofac wfrac skin

*GEOMETRY J 0.0762 0.249 1.0 0.0

PERF GEOA 'Pr-1'

** UBA	ff	Status	Connection	REFLAYER
11 5 1	1.0 OPEN	FLOW-TO	'SURFACE'	REFLAYER
11 5 2	1.0 OPEN	FLOW-TO	1	
11 5 3	1.0 OPEN	FLOW-TO	2	
11 5 4	1.0 OPEN	FLOW-TO	3	
11 5 5	1.0 OPEN	FLOW-TO	4	
11 6 5	1.0 OPEN	FLOW-TO	5	
11 6 6	1.0 OPEN	FLOW-TO	6	
11 6 7	1.0 OPEN	FLOW-TO	7	
11 6 8	1.0 OPEN	FLOW-TO	8	
11 6 9	1.0 OPEN	FLOW-TO	9	
11 6 10	1.0 OPEN	FLOW-TO	10	
11 7 10	1.0 OPEN	FLOW-TO	11	
11 7 11	1.0 OPEN	FLOW-TO	12	
11 7 12	1.0 OPEN	FLOW-TO	13	
11 7 13	1.0 OPEN	FLOW-TO	14	
11 7 14	1.0 OPEN	FLOW-TO	15	
11 8 14	1.0 OPEN	FLOW-TO	16	
10 8 14	1.0 OPEN	FLOW-TO	17	
10 9 14	1.0 OPEN	FLOW-TO	18	
10 9 13	1.0 OPEN	FLOW-TO	19	
10 9 12	1.0 OPEN	FLOW-TO	20	
10 9 11	1.0 OPEN	FLOW-TO	21	
10 9 10	1.0 OPEN	FLOW-TO	22	
10 9 9	1.0 OPEN	FLOW-TO	23	
10 9 8	1.0 OPEN	FLOW-TO	24	
10 9 7	1.0 OPEN	FLOW-TO	25	
10 9 6	1.0 OPEN	FLOW-TO	26	
10 9 5	1.0 OPEN	FLOW-TO	27	
10 9 4	1.0 OPEN	FLOW-TO	28	
10 9 3	1.0 OPEN	FLOW-TO	29	
10 10 3	1.0 OPEN	FLOW-TO	30	
10 10 2	1.0 OPEN	FLOW-TO	31	

*TIME 1

*TIME 365

*TIME 730

*PRODUCER 'Pr-1'

*OPERATE *STO 2192

**OPERATE *STL 4384

*OPERATE MIN BHP 1550.0 CONT

```

**          rad geofac wfrac skin
*GEOMETRY J 0.0762 0.249 1.0 0.0
  PERF      GEOA 'Pr-1'
** UBA      ff          Status Connection
   11 5 1    1.0 OPEN    FLOW-TO 'SURFACE' REFLAYER
   11 5 2    1.0 OPEN    FLOW-TO 1
   11 5 3    1.0 OPEN    FLOW-TO 2
   11 5 4    1.0 OPEN    FLOW-TO 3
   11 5 5    1.0 OPEN    FLOW-TO 4
   11 6 5    1.0 OPEN    FLOW-TO 5
   11 6 6    1.0 OPEN    FLOW-TO 6
   11 6 7    1.0 OPEN    FLOW-TO 7
   11 6 8    1.0 OPEN    FLOW-TO 8
   11 6 9    1.0 OPEN    FLOW-TO 9
   11 6 10   1.0 OPEN    FLOW-TO 10
   11 7 10   1.0 OPEN    FLOW-TO 11
   11 7 11   1.0 OPEN    FLOW-TO 12
   11 7 12   1.0 OPEN    FLOW-TO 13
   11 7 13   1.0 OPEN    FLOW-TO 14
   11 7 14   1.0 OPEN    FLOW-TO 15
   11 8 14   1.0 OPEN    FLOW-TO 16
   10 8 14   1.0 OPEN    FLOW-TO 17
   10 9 14   1.0 OPEN    FLOW-TO 18
   10 9 13   1.0 OPEN    FLOW-TO 19
   10 9 12   1.0 OPEN    FLOW-TO 20
   10 9 11   1.0 OPEN    FLOW-TO 21
   10 9 10   1.0 OPEN    FLOW-TO 22
   10 9 9    1.0 OPEN    FLOW-TO 23
   10 9 8    1.0 OPEN    FLOW-TO 24
   10 9 7    1.0 OPEN    FLOW-TO 25
   10 9 6    1.0 OPEN    FLOW-TO 26
   10 9 5    1.0 OPEN    FLOW-TO 27
   10 9 4    1.0 OPEN    FLOW-TO 28
   10 9 3    1.0 OPEN    FLOW-TO 29
   10 10 3   1.0 OPEN    FLOW-TO 30
   10 10 2   1.0 OPEN    FLOW-TO 31

```

```

*TIME 1095
*TIME 1460

```

```

*PRODUCER 'Pr-1'
*OPERATE *STO 2192
**OPERATE *STL 4384
*OPERATE MIN BHP 2400.0 CONT
**          rad geofac wfrac skin
*GEOMETRY J 0.0762 0.249 1.0 0.0
  PERF      GEOA 'Pr-1'
** UBA      ff          Status Connection
   11 5 1    1.0 OPEN    FLOW-TO 'SURFACE' REFLAYER
   11 5 2    1.0 OPEN    FLOW-TO 1
   11 5 3    1.0 OPEN    FLOW-TO 2
   11 5 4    1.0 OPEN    FLOW-TO 3
   11 5 5    1.0 OPEN    FLOW-TO 4
   11 6 5    1.0 OPEN    FLOW-TO 5
   11 6 6    1.0 OPEN    FLOW-TO 6
   11 6 7    1.0 OPEN    FLOW-TO 7
   11 6 8    1.0 OPEN    FLOW-TO 8
   11 6 9    1.0 OPEN    FLOW-TO 9
   11 6 10   1.0 OPEN    FLOW-TO 10
   11 7 10   1.0 OPEN    FLOW-TO 11

```

11 7 11	1.0	OPEN	FLOW-TO	12
11 7 12	1.0	OPEN	FLOW-TO	13
11 7 13	1.0	OPEN	FLOW-TO	14
11 7 14	1.0	OPEN	FLOW-TO	15
11 8 14	1.0	OPEN	FLOW-TO	16
10 8 14	1.0	OPEN	FLOW-TO	17
10 9 14	1.0	OPEN	FLOW-TO	18
10 9 13	1.0	OPEN	FLOW-TO	19
10 9 12	1.0	OPEN	FLOW-TO	20
10 9 11	1.0	OPEN	FLOW-TO	21
10 9 10	1.0	OPEN	FLOW-TO	22
10 9 9	1.0	OPEN	FLOW-TO	23
10 9 8	1.0	OPEN	FLOW-TO	24
10 9 7	1.0	OPEN	FLOW-TO	25
10 9 6	1.0	OPEN	FLOW-TO	26
10 9 5	1.0	OPEN	FLOW-TO	27
10 9 4	1.0	OPEN	FLOW-TO	28
10 9 3	1.0	OPEN	FLOW-TO	29
10 10 3	1.0	OPEN	FLOW-TO	30
10 10 2	1.0	OPEN	FLOW-TO	31

*TIME 1825
*TIME 2190

*PRODUCER 'Pr-1'
*OPERATE *STO 2192
**OPERATE *STL 4384
*OPERATE MIN BHP 2850.0 CONT
** rad geofac wfrac skin
*GEOMETRY J 0.0762 0.249 1.0 0.0
PERF GEOA 'Pr-1'

** UBA	ff	Status	Connection	
11 5 1	1.0	OPEN	FLOW-TO	'SURFACE' REFLAYER
11 5 2	1.0	OPEN	FLOW-TO	1
11 5 3	1.0	OPEN	FLOW-TO	2
11 5 4	1.0	OPEN	FLOW-TO	3
11 5 5	1.0	OPEN	FLOW-TO	4
11 6 5	1.0	OPEN	FLOW-TO	5
11 6 6	1.0	OPEN	FLOW-TO	6
11 6 7	1.0	OPEN	FLOW-TO	7
11 6 8	1.0	OPEN	FLOW-TO	8
11 6 9	1.0	OPEN	FLOW-TO	9
11 6 10	1.0	OPEN	FLOW-TO	10
11 7 10	1.0	OPEN	FLOW-TO	11
11 7 11	1.0	OPEN	FLOW-TO	12
11 7 12	1.0	OPEN	FLOW-TO	13
11 7 13	1.0	OPEN	FLOW-TO	14
11 7 14	1.0	OPEN	FLOW-TO	15
11 8 14	1.0	OPEN	FLOW-TO	16
10 8 14	1.0	OPEN	FLOW-TO	17
10 9 14	1.0	OPEN	FLOW-TO	18
10 9 13	1.0	OPEN	FLOW-TO	19
10 9 12	1.0	OPEN	FLOW-TO	20
10 9 11	1.0	OPEN	FLOW-TO	21
10 9 10	1.0	OPEN	FLOW-TO	22
10 9 9	1.0	OPEN	FLOW-TO	23
10 9 8	1.0	OPEN	FLOW-TO	24
10 9 7	1.0	OPEN	FLOW-TO	25
10 9 6	1.0	OPEN	FLOW-TO	26
10 9 5	1.0	OPEN	FLOW-TO	27

10 9 4	1.0	OPEN	FLOW-TO	28
10 9 3	1.0	OPEN	FLOW-TO	29
10 10 3	1.0	OPEN	FLOW-TO	30
10 10 2	1.0	OPEN	FLOW-TO	31

*TIME 2555
*TIME 2920

*PRODUCER 'Pr-1'
*OPERATE *STO 2192
**OPERATE *STL 4384
*OPERATE MIN BHP 3000.0 CONT
** rad geofac wfrac skin
*GEOMETRY J 0.0762 0.249 1.0 0.0
PERF GEOA 'Pr-1'

** UBA	ff	Status	Connection	
11 5 1	1.0	OPEN	FLOW-TO	'SURFACE' REFLAYER
11 5 2	1.0	OPEN	FLOW-TO	1
11 5 3	1.0	OPEN	FLOW-TO	2
11 5 4	1.0	OPEN	FLOW-TO	3
11 5 5	1.0	OPEN	FLOW-TO	4
11 6 5	1.0	OPEN	FLOW-TO	5
11 6 6	1.0	OPEN	FLOW-TO	6
11 6 7	1.0	OPEN	FLOW-TO	7
11 6 8	1.0	OPEN	FLOW-TO	8
11 6 9	1.0	OPEN	FLOW-TO	9
11 6 10	1.0	OPEN	FLOW-TO	10
11 7 10	1.0	OPEN	FLOW-TO	11
11 7 11	1.0	OPEN	FLOW-TO	12
11 7 12	1.0	OPEN	FLOW-TO	13
11 7 13	1.0	OPEN	FLOW-TO	14
11 7 14	1.0	OPEN	FLOW-TO	15
11 8 14	1.0	OPEN	FLOW-TO	16
10 8 14	1.0	OPEN	FLOW-TO	17
10 9 14	1.0	OPEN	FLOW-TO	18
10 9 13	1.0	OPEN	FLOW-TO	19
10 9 12	1.0	OPEN	FLOW-TO	20
10 9 11	1.0	OPEN	FLOW-TO	21
10 9 10	1.0	OPEN	FLOW-TO	22
10 9 9	1.0	OPEN	FLOW-TO	23
10 9 8	1.0	OPEN	FLOW-TO	24
10 9 7	1.0	OPEN	FLOW-TO	25
10 9 6	1.0	OPEN	FLOW-TO	26
10 9 5	1.0	OPEN	FLOW-TO	27
10 9 4	1.0	OPEN	FLOW-TO	28
10 9 3	1.0	OPEN	FLOW-TO	29
10 10 3	1.0	OPEN	FLOW-TO	30
10 10 2	1.0	OPEN	FLOW-TO	31

*TIME 3285
*TIME 3650
*STOP

APPENDIX B

Surfactant Imbibition 0.1% concentration (30-15-90) Simulation Code:

```
SHUTIN 'Pr-1'
OPEN 'In-1'
*INJECTOR 'In-1'
  *incomp *water 0.999 0.001 0.000 0
  *TINJW 95
  *OPERATE MAX *BHP 4000 ** Start on BHP
  **OPERATE *MAX *STW 484.56 *CONT REPEAT** 0.2PV/2733400/13667000 **
Maximum water rate
*TIME 3680
SHUTIN 'Pr-1'
SHUTIN 'In-1'

*TIME 3695
SHUTIN 'In-1'
OPEN 'Pr-1'
  *PRODUCER 'Pr-1'
  *OPERATE *MIN BHP 550
  **OPERATE *STO 161.52 ** Maximum liquid rate **0.89ml/day

*TIME 3785
SHUTIN 'Pr-1'
OPEN 'In-1'

*TIME 3815
SHUTIN 'Pr-1'
SHUTIN 'In-1'

*TIME 3830
SHUTIN 'In-1'
OPEN 'Pr-1'

*TIME 3920
SHUTIN 'Pr-1'
OPEN 'In-1'

*TIME 3950
SHUTIN 'Pr-1'
SHUTIN 'In-1'

TIME 3965
SHUTIN 'In-1'
OPEN 'Pr-1'

*TIME 4055
SHUTIN 'Pr-1'
OPEN 'In-1'

*TIME 4085
```

SHUTIN 'Pr-1'
SHUTIN 'In-1'

*TIME 4100
SHUTIN 'In-1'
OPEN 'Pr-1'

*TIME 4190
SHUTIN 'Pr-1'
OPEN 'In-1'

*TIME 4220
SHUTIN 'Pr-1'
SHUTIN 'In-1'

*TIME 4235
SHUTIN 'In-1'
OPEN 'Pr-1'

*TIME 4325
SHUTIN 'Pr-1'
OPEN 'In-1'

*TIME 4355
SHUTIN 'Pr-1'
SHUTIN 'In-1'

*TIME 4370
SHUTIN 'In-1'
OPEN 'Pr-1'

*TIME 4460
SHUTIN 'Pr-1'
OPEN 'In-1'

*TIME 4490
SHUTIN 'Pr-1'
SHUTIN 'In-1'

*TIME 4505
SHUTIN 'In-1'
OPEN 'Pr-1'

*TIME 4595
SHUTIN 'Pr-1'
OPEN 'In-1'

*TIME 4625
SHUTIN 'Pr-1'
SHUTIN 'In-1'

*TIME 4640
SHUTIN 'In-1'
OPEN 'Pr-1'

*TIME 4730
SHUTIN 'Pr-1'
OPEN 'In-1'

*TIME 4760

SHUTIN 'Pr-1'
SHUTIN 'In-1'

*TIME 4775
SHUTIN 'In-1'
OPEN 'Pr-1'

*TIME 4865
SHUTIN 'Pr-1'
OPEN 'In-1'

*TIME 4895
SHUTIN 'Pr-1'
SHUTIN 'In-1'

TIME 4910
SHUTIN 'In-1'
OPEN 'Pr-1'

*TIME 5000
SHUTIN 'Pr-1'
OPEN 'In-1'

*TIME 5030
SHUTIN 'Pr-1'
SHUTIN 'In-1'

*TIME 5045
SHUTIN 'In-1'
OPEN 'Pr-1'

*TIME 5135
SHUTIN 'Pr-1'
OPEN 'In-1'

*TIME 5165
SHUTIN 'Pr-1'
SHUTIN 'In-1'

*TIME 5180
SHUTIN 'In-1'
OPEN 'Pr-1'

*TIME 5270
SHUTIN 'Pr-1'
OPEN 'In-1'

*TIME 5300
SHUTIN 'Pr-1'
SHUTIN 'In-1'

*TIME 5315
SHUTIN 'In-1'
OPEN 'Pr-1'

*TIME 5405
SHUTIN 'Pr-1'
OPEN 'In-1'

*TIME 5435

SHUTIN 'Pr-1'
SHUTIN 'In-1'

*TIME 5450
SHUTIN 'In-1'
OPEN 'Pr-1'

*TIME 5540
SHUTIN 'Pr-1'
OPEN 'In-1'

*TIME 5570
SHUTIN 'Pr-1'
SHUTIN 'In-1'

*TIME 5585
SHUTIN 'In-1'
OPEN 'Pr-1'

*TIME 5675
SHUTIN 'Pr-1'
OPEN 'In-1'

*TIME 5705
SHUTIN 'Pr-1'
SHUTIN 'In-1'

*TIME 5720
SHUTIN 'In-1'
OPEN 'Pr-1'

*TIME 5810
SHUTIN 'Pr-1'
OPEN 'In-1'

*TIME 5840
SHUTIN 'Pr-1'
SHUTIN 'In-1'

TIME 5855
SHUTIN 'In-1'
OPEN 'Pr-1'

*TIME 5945
SHUTIN 'Pr-1'
OPEN 'In-1'

*TIME 5975
SHUTIN 'Pr-1'
SHUTIN 'In-1'

*TIME 5990
SHUTIN 'In-1'
OPEN 'Pr-1'

*TIME 6080
SHUTIN 'Pr-1'
OPEN 'In-1'

*TIME 6110

SHUTIN 'Pr-1'
SHUTIN 'In-1'

*TIME 6125
SHUTIN 'In-1'
OPEN 'Pr-1'

*TIME 6215
SHUTIN 'Pr-1'
OPEN 'In-1'

*TIME 6245
SHUTIN 'Pr-1'
SHUTIN 'In-1'

*TIME 6260
SHUTIN 'In-1'
OPEN 'Pr-1'

*TIME 6350
SHUTIN 'Pr-1'
OPEN 'In-1'

*TIME 6380
SHUTIN 'Pr-1'
SHUTIN 'In-1'

*TIME 6395
SHUTIN 'In-1'
OPEN 'Pr-1'

*TIME 6485
SHUTIN 'Pr-1'
OPEN 'In-1'

*TIME 6515
SHUTIN 'Pr-1'
SHUTIN 'In-1'

*TIME 6530
SHUTIN 'In-1'
OPEN 'Pr-1'

*TIME 6620
SHUTIN 'Pr-1'
OPEN 'In-1'

*TIME 6650
SHUTIN 'Pr-1'
SHUTIN 'In-1'

*TIME 6665
SHUTIN 'In-1'
OPEN 'Pr-1'

*TIME 6755
SHUTIN 'Pr-1'
OPEN 'In-1'

*TIME 6785

SHUTIN 'Pr-1'
SHUTIN 'In-1'

TIME 6800
SHUTIN 'In-1'
OPEN 'Pr-1'

*TIME 6890
SHUTIN 'Pr-1'
OPEN 'In-1'

*TIME 6920
SHUTIN 'Pr-1'
SHUTIN 'In-1'

*TIME 6935
SHUTIN 'In-1'
OPEN 'Pr-1'

*TIME 7025
SHUTIN 'Pr-1'
OPEN 'In-1'

*TIME 7055
SHUTIN 'Pr-1'
SHUTIN 'In-1'

*TIME 7070
SHUTIN 'In-1'
OPEN 'Pr-1'

*TIME 7160
SHUTIN 'Pr-1'
OPEN 'In-1'

*TIME 7190
SHUTIN 'Pr-1'
SHUTIN 'In-1'

*TIME 7205
SHUTIN 'In-1'
OPEN 'Pr-1'

*TIME 7300
*STOP

APPENDIX C

Table of all wells used for geological modeling:

file_no	api_no	operator	well_name	td	field_name	latitude	longitude	well_type	status	symbol
23565	33-061-02224-00-00	WHITING OIL AND GAS CORPORATION	MCNAMARA 41-26XH	20342	SANISH	48.05121651	-102.3325107	OG	A	OG
17364	33-061-00773-00-00	LIME ROCK RESOURCES III-A, L.P.	REUM 11-32H	15500	STANLEY	48.20975362	-102.4157223	OG	A	OG
17410	33-061-00788-00-00	EOG RESOURCES, INC.	BURKE 3-16H	14450	STANLEY	48.25360196	-102.2656799	OG	A	OG
16824	33-061-00577-00-00	HESS BAKKEN INVESTMENTS II, LLC	RS-NELSON-156-91 1423H-1	19041	ROSS	48.33990833	-102.3513511	OG	A	OG
99186	33-061-99186-00-00	EOG RESOURCES, INC.	SIDONIA 100-06	9042	CLEAR WATER	48.54015277	-102.3498039	SWD	A	SWD
17043	33-061-00653-00-00	HESS BAKKEN INVESTMENTS II, LLC	ST-ANDES-151-89- 2413H-1	19258	BANNER	47.87729922	-102.001518	OG	IA	OG
99188	33-061-99188-00-00	EOG RESOURCES, INC.	LIBERTY 22-12M	10447	VAN HOOK	47.91212463	-102.2666725	ST	DRY	DRY
21928	33-061-01923-00-00	MUREX PETROLEUM CORPORATION	JUNIOR 10-3H	18395	SANISH	48.16858601	-102.3551079	OG	A	OG
16743	33-061-00557-00-00	EOG RESOURCES, INC.	FERTILE 1-12 SWD	15313	PARSHALL	47.90635849	-102.1298284	SWD	A	SWD
17058	33-061-00660-00-00	EOG RESOURCES, INC.	SHELL CREEK 1-01 SWD	13459	PARSHALL	48.00926076	-102.1419641	SWD	A	SWD
15845	33-061-00489-00-00	HESS BAKKEN INVESTMENTS II, LLC	NELSON FARMS 1-24H	14433	ROSS	48.3135595	-102.4401633	OG	IA	OG
16532	33-061-00521-00-00	EOG RESOURCES, INC.	N&D 1-05H	14900	PARSHALL	48.02185641	-102.222582	OG	A	OG
16324	33-061-00503-00-00	EOG RESOURCES, INC.	PARSHALL 2-36H	12111	PARSHALL	48.03686527	-102.1996905	OG	A	OG
17780	33-061-00912-00-00	EOG RESOURCES, INC.	CROWFOOT 1-17H	13652	CLEAR WATER	48.51667029	-102.210255	OG	A	OG
16799	33-061-00571-00-00	HUNT OIL COMPANY	PATTEN 1-27H	13771	PARSHALL	48.03822177	-102.101366	OG	A	OG
16862	33-061-00587-00-00	LANDTECH ENTERPRISES, LLC	BLOOM SWD 1	12608	WILDCAT	48.26998025	-102.143348	SWD	A	SWD
16733	33-061-00554-00-00	EOG RESOURCES, INC.	WAYZETTA 100-26 SWD	9580	PARSHALL	48.0438492	-102.2167749	SWD	A	SWD
16885	33-061-00596-00-00	EOG RESOURCES, INC.	AUSTIN 8-26H	14843	PARSHALL	48.13809118	-102.222582	OG	A	OG
17071	33-061-00666-00-00	HESS BAKKEN INVESTMENTS II, LLC	RS-STATE C-157-90- 3603H-1	19718	ROSS	48.38631549	-102.2532015	OG	A	OG
17676	33-061-00884-00-00	EOG RESOURCES, INC.	SIDONIA 1-06H	13992	CLEAR WATER	48.53303243	-102.3443921	OG	A	OG
16997	33-061-00630-00-00	EOG RESOURCES, INC.	VAN HOOK 1-13H	14670	VAN HOOK	47.99095049	-102.277183	OG	A	OG
17023	33-061-00641-00-00	WHITING OIL AND GAS CORPORATION	BRAAFLAT 11-11H	19678	SANISH	48.09489323	-102.3507478	OG	A	OG
26661	33-061-02766-00-00	EOG RESOURCES, INC.	WAYZETTA 46-11M	10180	PARSHALL	48.09415704	-102.2123232	ST	DRY	DRY
21231	33-061-01826-00-00	XTO ENERGY INC.	JOHNSON 31-17SWH	0	WILDCAT	48.5161636	-102.0687721	OG	DRY	DRY
27850	33-061-03003-00-00	EOG RESOURCES, INC.	PARSHALL 408-15M	9787	PARSHALL	47.98583152	-102.1767107	ST	DRY	DRY

file_no	api_no	operator	Township	Range	SEC_1	QQ_1	HoleType	FirstSpudD	MeasuredTD	KBElev	MMDLP	MDB	DTF
23565	33-061-02224-00-00	WHITING OIL AND GAS CORPORATION	153	91	26	NENE	Horizontal	2012-10-01	20342	2181	8993	9784	9890
17364	33-061-00773-00-00	LIME ROCK RESOURCES III-A, L.P.	155	91	32	NWNW	Horizontal	2008-08-28	15500	2277	9044	9792	9892
17410	33-061-00788-00-00	EOG RESOURCES, INC.	155	90	16	NWNW	Horizontal	2008-09-07	14450	2326	8592	9312	9396
16824	33-061-00577-00-00	HESS BAKKEN INVESTMENTS II, LLC	156	91	14	NWNW	Horizontal	2007-10-19	19041	2252	8513	9197	9287
99186	33-061-99186-00-00	EOG RESOURCES, INC.	158	90	6	SWNE	Verticle	2009-04-08	9042	2329	8095	8707	8802
17043	33-061-00653-00-00	HESS BAKKEN INVESTMENTS II, LLC	151	89	24	SESE	Horizontal	2008-07-22	19258	2146	8306	9070	9137
99188	33-061-99188-00-00	EOG RESOURCES, INC.	151	91	12	NWSE	Verticle	2010-08-03	10447	2224	8832	9635	9728
21928	33-061-01923-00-00	MUREX PETROLEUM CORPORATION	154	91	10	SESE	Horizontal	2012-01-10	18395	2357	9074	9809	9909
16743	33-061-00557-00-00	EOG RESOURCES, INC.	151	90	12	SESE	Horizontal	2007-08-26	15313	2130	8586	9360	9440
17058	33-061-00660-00-00	EOG RESOURCES, INC.	152	90	1	SESW	Directional	2008-02-12	13459	2112	8427	9187	9270
15845	33-061-00489-00-00	HESS BAKKEN INVESTMENTS II, LLC	156	92	24	SESE	Horizontal	2005-07-14	14433	2350	8900	9596	9689
16532	33-061-00521-00-00	EOG RESOURCES, INC.	152	90	5	LOT3	Horizontal	2007-04-14	14900	2081	8638	9413	9500
16324	33-061-00503-00-00	EOG RESOURCES, INC.	153	90	36	NWNW	Horizontal	2006-08-03	12111	2042	8502	9268	9354
17780	33-061-00912-00-00	EOG RESOURCES, INC.	158	89	17	NWNW	Horizontal	2008-11-16	13652	2313	7753	8397	8463
16799	33-061-00571-00-00	HUNT OIL COMPANY	153	89	27	SWSE	Horizontal	2007-12-14	13771	2134	8296	9050	9132
16862	33-061-00587-00-00	LANDTECH ENTERPRISES, LLC	155	89	5	SWSE	Horizontal	2007-11-11	12608	2173	7743	8803	8872
16733	33-061-00554-00-00	EOG RESOURCES, INC.	153	90	26	NESW	Verticle	2007-10-24	9580	2132	8622	9380	9468
16885	33-061-00596-00-00	EOG RESOURCES, INC.	154	90	26	NWNW	Horizontal	2007-11-22	14843	2236	8611	9365	9450
17071	33-061-00666-00-00	HESS BAKKEN INVESTMENTS II, LLC	157	90	36	NWNW	Horizontal	2008-03-18	19718	2269	8100	8773	8846
17676	33-061-00884-00-00	EOG RESOURCES, INC.	158	90	6	SESE	Horizontal	2008-10-19	13992	2313	8094	8721	8794
16997	33-061-00630-00-00	EOG RESOURCES, INC.	152	91	13	NWNW	Horizontal	2008-03-22	14670	1962	8692	9490	9590
17023	33-061-00641-00-00	WHITING OIL AND GAS CORPORATION	153	91	11	NWNW	Horizontal	2008-03-10	19678	2299	9076	9865	9972
26661	33-061-02766-00-00	EOG RESOURCES, INC.	153	90	11	NWNE	Verticle	2013-11-11	10180	2202	8593	9350	9435
21231	33-061-01826-00-00	XTO ENERGY INC.	158	88	17	NWNE	Horizontal	2011-10-10	0	2294	7564	8037	8102
27850	33-061-03003-00-00	EOG RESOURCES, INC.	152	90	15	SENE	Directional	2014-04-12	9787	2045	8532	9290	9372